OXFORD CDE

Journal of Computational Design and Engineering, 2022, 9(3), 1135–1156

https://doi.org/10.1093/jcde/qwac042
Journal homepage: www.jcde.org

RESEARCH ARTICLE

Developing an integrated model for planning the delivery of construction materials to post-disaster reconstruction projects

Zahra Gharib[1], Maziar Yazdani[2,*], Ali Bozorgi-Amiri[3], Reza Tavakkoli-Moghaddam[3] and Mohammad Javad Taghipourian[4]

[1]School of Industrial Engineering, College of Engineering, University of Tehran, Tehran 1439957131, Iran; [2]School of Civil & Environmental Engineering, University of New South Wales, Sydney 2052, Australia; [3]School of Industrial Engineering, College of Engineering, University of Tehran, Tehran 1439957131, Iran and [4]Department of Business Management, Chalous Branch, Islamic Azad University, Chalous 46615/397, Iran

*Corresponding author. E-mail: maziar.yazdani@unsw.edu.au https://orcid.org/0000-0001-9462-5439

Abstract

Construction material delivery to post-disaster reconstruction projects is challenging because of the resource and time limitations that follow a large-scale disaster. There is compelling evidence that inadequate planning jeopardises the success of a large number of post-disaster reconstruction projects. Thus, the current study proposes an integrated approach to facilitate the procurement planning of construction materials following a large-scale disaster. The proposed approach clustered the location of construction projects using a differential evolution (DE)-K-prototypes, a new partitional clustering algorithm based on DE and K-prototypes, method. Then, using a permanent matrix prioritises cluster points based on route reliability-affecting factors. The model's objectives are to minimise the total travel time, maximise the reliability of the route, and minimise the total weighted undelivered materials to projects. In the case of distribution of material through land vehicles, the possibility of breakdowns in the vehicle is considered, allowing for the determination of vehicle breakdown under various scenarios and the minimisation of undelivered materials to projects. As a result of the uncertain character of the disaster, the demands of construction projects are fuzzy, and Jimenez's method is used to handle it. Due to the complexity of the problem, two algorithms are proposed, a multi-objective evolutionary algorithm based on decomposition (MOEA/D) and a non-dominated sorting genetic algorithm-II (NSGA-II). The results confirm that the proposed MOEA/D has a higher accuracy while NSGA-II has a shorter computational time. By providing new theoretical perspectives on disaster recovery strategies in the construction sector, this study contributes to the growing body of knowledge about disaster recovery strategies in the sector. The findings of this study can be employed to develop an integrated planning system for the delivery of construction materials to post-disaster reconstruction projects in disaster-prone countries.

Keywords: post-disaster reconstruction; non-dominated sorting genetic algorithm-II; post disaster; construction material; multi-objective evolutionary algorithm based on decomposition; augmented ε-constraint method

Received: 21 February 2022; **Revised:** 13 April 2022; **Accepted:** 26 April 2022

1. Introduction

Almost four-fifths of the world's cities are located in disaster-prone areas (Celentano *et al.*, 2019). Climate change is expected to exacerbate many types of natural disasters, particularly extreme weather events, with low-income countries bearing the brunt of the impact (Yazdani *et al.*, 2022). Disaster-related losses are more tangible in less developed regions (Dulebenets *et al.*, 2019). Disasters have a 20-fold greater impact on the built environment in developing countries than in developed countries (Barakat, 2003), owing to widespread substandard construction, leaving many people in need of housing in countries that are already struggling with their daily economies and housing challenges (Uddin & Matin, 2021).

Disaster recovery efforts prioritise the reconstruction of houses and public infrastructure (Rouhanizadeh & Kermanshachi, 2020). Effective delivery has become a significant issue when it comes to large-scale post-disaster reconstruction projects (Safapour & Kermanshachi, 2021). In the aftermath of a disaster, reconstruction must deal with the conflicting demands of the displaced population and the need for agencies to plan programmes that address both the immediate need for shelter and the long-term need for permanent housing (Bahmani & Zhang, 2021b). This longer term plan is intended to accommodate not only a socioeconomic recovery but possibly an improvement over pre-disaster conditions, as recommended by the Sendai agreement and the globally adopted building back better reconstruction guidelines (Habibi Rad *et al.*, 2021a). Meanwhile, the spontaneous tendency of the population is to rush into restoring livelihood "back to normal," often ending up replicating previous vulnerability by building in disaster-prone areas or using unsafe construction methods (Platt & So, 2017). As a result, this circumstance puts pressure on authorities and agencies to deliver a response that may meet the required speed while failing on socioeconomic aspects (Bahmani & Zhang, 2021a). It is important to draw the importance of providing a quick recovery in order to avoid the establishment of unsafe building structures (Habibi Rad *et al.*, 2021b).

Post-disaster reconstruction projects face challenges that go beyond standard construction issues and are prone to delivering inadequate building solutions (Siriwardhana *et al.*, 2021). This is directly related to the need for quick reaction time in stressful situations (Mahtab *et al.*, 2021). Although these circumstances are well known, the strategies required to overcome these difficulties appear to be less clear (Bahmani & Zhang, 2022b). Some issues have been identified as major bottlenecks in reconstruction projects, including supply chain planning challenges and resource shortages (Celentano *et al.*, 2019). Solutions to overcome these obstacles are still being discussed (Huang *et al.*, 2021). Bilau *et al.* (2017) indicate challenges associated with logistics and supplies as one of the major management issues that arise in large-scale housing reconstruction programmes.

Construction materials and their supply chain in post-disaster reconstruction projects can be linked to many bottlenecks (Chang *et al.*, 2010). After a destructive disaster, the majority of local manufacturing facilities and supply systems in manufacturing industries are likely to be damaged, causing havoc in the construction market. This also results in price fluctuations (Khodahemmati & Shahandashti, 2020). Numerous international organisations, including the IFRC and UN agencies, have also emphasised the importance of resource availability as a critical factor in optimising recovery efforts (Celentano *et al.*, 2019). The majority of research in the field of post-disaster reconstruction is limited to certain social science perspectives or examinations of prior experiences. For example, Enshassi *et al.* (2017) explored factors influencing post-disaster reconstruction project management for housing provision in the Gaza Strip. Bahmani and Zhang (2021b) proposed a success evaluation framework consisting of a definition of the successful recovery measurements and how influential factors can be used to manage socio-natural disaster recovery projects. Mohammadnazari *et al.* (2022) presented an integrated approach based on four multi-criteria decision-making techniques: TOPSIS, ELECTRE III, VIKOR, and PROMETHEE, to aid decision makers in prioritizing post-disaster projects. Copping *et al.* (2022) investigated the supply networks of construction materials for disaster-relief shelters and reconstruction. A questionnaire was used to collect the data. The sample consisted of 272 displaced families from four countries (Nepal, Bangladesh, Afghanistan, and Turkey). The data were analysed using social network analysis. Charles *et al.* (2022) reviewed the literature on resilience factors used in post-disaster reconstruction projects and formed a framework to aid in strategic selection and application. Habibi Rad *et al.* (2022) proposed a conceptual framework for implementing lean construction in infrastructure recovery projects. Bahmani and Zhang (2022a) conducted a study to simplify the disaster recovery project management procedure by identifying common activities and assigning them to appropriate places based on the disaster recovery project's timeline.

However, few studies in this field have addressed the modelling approach. For example, Xu *et al.* (2019), Xiong *et al.* (2020), and Ghannad *et al.* (2020) proposed methods such as genetic algorithm and priority indices to determine the reconstruction order of buildings. Ghannad *et al.* (2021) developed a prioritisation approach for rapid and optimised post-disaster recovery that evaluates recovery priorities of damaged transportation infrastructure systems and affected regions through a multi-agent system using a reinforcement learning technique. Zokaee *et al.* (2021) developed a multi-resource, capacitated tour covering location-routing model to design a post-disaster reconstruction supply chain considering disruption risk during the recovery phase to minimise total costs by determining optimal locations of temporary resource distribution warehouses and optimal paths for transferring reconstruction resources to the impacted areas. Gharib *et al.* (2022) developed an integrated model for the distribution of post-disaster temporary shelters after a large-scale disaster. Huang *et al.* (2022) established a research framework for efficiently and comprehensively modelling and assessing post-disaster economic losses that can be used to analyse the full supply chain losses caused by other disasters with data availability and reliability or to simulate the full economic losses caused by an unexpected event in order to improve decision makers' disaster management and response capacity. Diaz *et al.* (2022) evaluated supply, costs, and recovery times using a combination of Monte Carlo and beta models. The proposed models incorporate stochastic components into projected material, labour, and equipment flows to capture reconstruction activities' immediate and long-term costs under highly uncertain conditions. The model could identify potential roadblocks in obtaining necessary materials and labour and prospective thresholds that could impede the housing recovery process. Alisjahbana *et al.* (2022) proposed a method for determining reconstruction policies and strategies, particularly for interdependent building systems like the school system. They discussed the situation of post-disaster school reconstruction, in which students are relocated to the nearest functional school if their original school was damaged. The objective of the problem was to determine the order in which damaged schools should be reconstructed by minimising the sum of the distance all students in the region have to travel until all schools in the region are reconstructed.

Despite recent advancements in different phases of disaster risk management plans and strategies (Dulebenets *et al*., 2019; Abioye *et al*., 2020; Chen *et al*., 2022), mathematical and optimisations' approaches have not adequately addressed the issues of post-disaster reconstructions and the challenges and obstacles faced by recovery projects (Tirkolaee *et al*., 2020a). As a result, this research's primary aim is to develop an integrated optimisation model for post-disaster recovery planning to enable the most efficient use of scarce construction resources caused by natural disasters. The proposed model clusters the location of construction projects by using the proposed differential evolution (DE)-K-prototypes method and then prioritises the points of clusters by affecting factors on the route reliability using a permanent matrix. The model's objectives are to minimise the total travel time, maximise the reliability of the route, and minimise the total weighted undelivered materials to projects. Furthermore, the possibility of the breakdown in the vehicle is considered in the model. Considering the uncertainties associated with post-disaster reconstruction, the demands for materials in each project are fuzzy. As the problem is complex, two multi-objective meta-heuristic algorithms, non-dominated sorting genetic algorithm-II (NSGA-II) and multi-objective evolutionary algorithm based on decomposition (MOEA/D), are proposed to solve the problem.

2. Contributions

The review of the literature reveals that procurement issues in post-disaster reconstruction projects are still unresolved and unexplored. Many questions about formulation parameters and assumptions remain unanswered in existing studies, which can only be viewed as preliminary steps towards a more comprehensive understanding of post-disaster construction project planning. The main contributions of this study can be stated as follows:

(i) **Clustering construction sites before designing the mathematical model and the formation of the routing network in order to accelerate the distribution of construction materials:** Consideration of the location of construction projects with geographically common features, spatial features, and other factors in a cluster (assuming that the paths leading to those locations are impacted) can have a significant impact on accelerating and improving material distribution performance. Furthermore, the safety of material delivery operations to a construction site is critical. This study investigates the identification of common factors and features for clustering the location of construction projects in light of route disruption. Clustering is accomplished using the proposed DE-K-prototypes method in this study. In the DE-K-prototypes model, after identifying and collecting data, the factors are entered as model input, and the model considers important factors for clustering and places the most similar and relevant points in a cluster based on the type of training it has already seen.

(ii) **Prioritisation of construction projects based on effective factors of road safety in each cluster of construction project locations:** The majority of research in the field of crisis transportation and routeing focuses on the design of routeing networks and direct distribution of materials and goods with little regard for safety and reliability. Decisions in each cluster are made using a combination of graph theory and permanent matrix theory. The priority determined by this method selects the most reliable routes for delivering materials to construction projects.

(iii) **Multi-mode transportation system:** Considering two different modes of transportation in this study, both land and aerial vehicles, provides flexibility for the plan to serve locations with inaccessible routes. Even in the event of secondary crises in material delivery operations, such as road disruption or adverse weather, delivery operations can be completed quickly and accurately on a scheduled basis.

(iv) **Simultaneous consideration of routing factors such as heterogeneity of vehicles, multiple warehouses of the routing network, multi-period distribution of materials, and multi-type of construction materials:** Using the same type of vehicle (homogeneous vehicle) may impact adversely the performance of planning to distribute materials and respond quickly to the construction projects, so consider vehicles that differ in capacity, speed, fuel consumption, and so on (heterogeneous vehicles), which may provide flexibility for providing materials to different construction projects in different locations with different demands. This will solve the issue. On the other hand, the distribution network's multi-warehouse structure can save time in serving construction projects.

(v) **Consider the disruption in the vehicle operation:** Emergency situations can cause a variety of disruptions, such as traffic, vehicle breakdowns, and other issues given the scale and duration of the rescue efforts. Undelivered materials to projects have resulted because some construction projects cannot receive services.

(vi) **Considering the uncertainty in demand for construction projects:** Due to the uncertain nature of the disasters, it is reasonable to consider some effective parameters of the uncertain routeing model, such as warehouse capacity and vehicle costs for on-demand transportation. Due to the fact that demand in affected areas is high and uncertain during a disaster, the uncertainty associated with the demand parameter is considered fuzzy in this study. We will work to alleviate the distribution system's uncertainty.

(vii) **Using several multi-objective methods:** The epsilon-constraint method is developed to solve the proposed mathematical model in a small-size problem. However, due to the complexity of the problem, two algorithms are proposed for the large-size problems, including the NSGA-II and a MOEA/D.

3. Proposed Framework for Planning the Delivery of Construction Materials

The three steps below outline the procedure for this study. Step 1 involves clustering and prioritising construction projects' locations, while Step 2 entails providing all stages of the mathematical model. Two multi-objective meta-heuristic algorithms, including NSGA-II and MOEA/D, are then used to solve the considered model. The proposed approach for planning the delivery of construction materials to post-disaster reconstruction projects is depicted schematically in Fig. 1.

3.1 Clustering the location of construction projects using DE-K-prototypes

By clustering the location of construction projects, response strategies for sending construction materials to these areas can

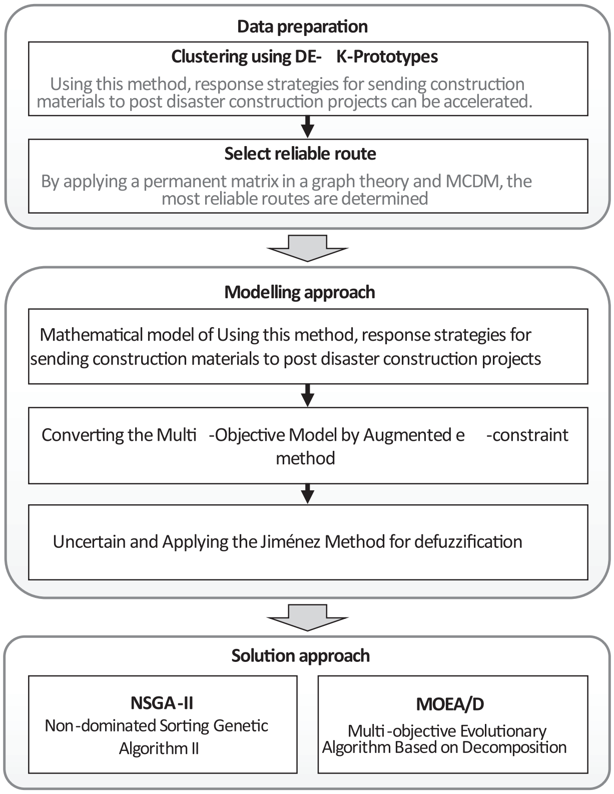

Figure 1: The proposed approach for planning the delivery of construction materials to post-disaster reconstruction projects.

be accelerated. To avoid getting stuck in local optima when clustering mixed numeric and categorical data, we propose DE-K-prototypes, a new partitional clustering algorithm based on DE and K-prototypes that avoids this problem by solving global optimisation problems instead of local ones. In this study, similar to (Ji *et al.*, 2020), a hybrid method is employed to cluster the data.

3.1.1 *The K-prototypes algorithm*

To cluster data with both numerical and categorical attributes, Huang (1997) introduced the k-prototypes algorithm. According to this algorithm, the dataset $\mathcal{X}$ should be partitioned into $\mathfrak{k}$ distinct clusters by minimising a below cost function:

$$E\left(\mathcal{U}, \mathcal{Z}\right) = \sum_{\mathfrak{l}=1}^{\mathfrak{k}} \sum_{\mathfrak{i}=1}^{n} \mathfrak{u}_{\mathfrak{i}\mathfrak{l}}\, \mathfrak{d}\left(\mathfrak{x}_{\mathfrak{i}}, \mathcal{Z}_{\mathfrak{l}}\right),\ \ 0 \le \mathfrak{u}_{\mathfrak{i}\mathfrak{l}} \le 1, \tag{1}$$

where $\mathcal{Z}_{\mathfrak{l}}$ denotes the prototype of the cluster $\mathfrak{l}$; $\mathfrak{u}_{\mathfrak{i}\mathfrak{l}}$ denotes an element of the partition matrix $U_{n\times k}$; and $d(\mathfrak{x}_{\mathfrak{i}}, \mathcal{Z}_{\mathfrak{l}})$ denotes the dissimilarity measure as follows:

$$\mathfrak{d}\left(\mathfrak{x}_{\mathfrak{i}}, \mathcal{Z}_{\mathfrak{l}}\right) = \sum_{\mathfrak{j}=1}^{m} \mathfrak{d}\left(\mathfrak{x}_{\mathfrak{i}\mathfrak{j}}, \mathfrak{z}_{\mathfrak{l}\mathfrak{j}}\right). \tag{2}$$

In the above formula, $\mathfrak{d}(\mathfrak{x}_{\mathfrak{i}\mathfrak{j}},\ \mathfrak{z}_{\mathfrak{l}\mathfrak{j}})$ is formulated as:

$$\mathfrak{d}\left(\mathfrak{x}_{\mathfrak{i}\mathfrak{j}}, \mathfrak{z}_{\mathfrak{l}\mathfrak{j}}\right) = \begin{cases} \left(\mathfrak{x}_{\mathfrak{i}\mathfrak{j}} - \mathfrak{z}_{\mathfrak{l}\mathfrak{j}}\right)^2, & \text{if the } \mathfrak{l}\text{th attribute is numeric,} \\ \mu_l \delta\left(\mathfrak{x}_{\mathfrak{i}\mathfrak{j}}, \mathfrak{z}_{\mathfrak{l}\mathfrak{j}}\right), & \text{if the } \mathfrak{l}\text{th attribute is categorical,} \end{cases} \tag{3}$$

where $\delta(\mathfrak{p}, \mathfrak{q}) = 0$ if $\mathfrak{p}$ and $\mathfrak{q}$ have the same value; $\delta(\mathfrak{p}, \mathfrak{q}) = 1$ if $\mathfrak{p}$ and $\mathfrak{q}$ have different values; $\mu_{\mathfrak{l}}$ denotes the weight assigned to categorical attributes within the cluster l. If the jth attribute is numeric, $\mathfrak{z}_{\mathfrak{l}\mathfrak{j}}$ represents the mean of the $\mathfrak{j}$th numeric attribute in the cluster $\mathfrak{l}$; if the $\mathfrak{j}$th attribute is categorical, $\mathfrak{z}_{\mathfrak{l}\mathfrak{j}}$ represents the mode of the $\mathfrak{j}$th categorical attribute in the cluster $\mathfrak{l}$. The k-prototypes algorithm is implemented as follows:

(i) Generate prototypes of clusters by selecting k random data points from the dataset $\mathcal{X}$.
(ii) Each data point in dataset $\mathcal{X}$ should be assigned to the cluster with the nearest prototype in accordance with Equation (2). After each allocation, make an update to the prototype cluster.
(iii) After allocating all data objects, re-evaluate their similarity to the current prototypes. If it is discovered that the nearest prototype of a data object is in a different cluster than the current one, reallocate the data object to that cluster and update the prototypes for both clusters.
(iv) If no data objects have changed clusters as a result of a full circle test of $\mathcal{X}$, the algorithm should be terminated; otherwise, proceed to Step III.

3.1.2 *The clustering algorithm based on DE and K-prototypes*

DE begins by generating an initial set of solutions (N) within the search space. Each individual in generation G is represented by a D-dimensional real-valued vector $X_i^G = (x_{i,1}^G,\ x_{i,2}^G,\ x_{i,3}^G,\ \ldots,\ x_{i,\ D}^G)$, where $i\ =\ 1, 2, 3,\ \ \ldots,\ N$. Following the initialisation phase, solutions are evolved and trial vectors are generated using mutation and crossover operators. Then, parents are compared to their corresponding trial vector, and the next generation's solutions are chosen at this stage (Yazdani *et al.*, 2021). Performing DE involves the following steps.

DE's population is made up of N individuals. DE typically begins with a randomly generated population, with the parameters of the i-th member of that population being generated as follows:

$$x_{i,j}^0 = x_j^{low}\ + rand\ \times \left(x_j^{up} - x_j^{low}\right),\ \ j\ =\ 1, 2, 3, \ldots, D \tag{4}$$

where D denotes the number of decision variables, and rand returns a uniformly distributed random number within the range [0,1]. Additionally, x_j^{low} and x_j^{up} denote the lower and upper bounds of solutions in the jth-dimensional search space, respectively. DE then uses the mutation procedure to generate mutant vectors after initialisation has taken place. In this section, "current-to-best/1:" $V_i^G = X_i^G\ + F.(X_{best}^G - X_{r1}^G) + F.(X_{r2}^G - X_{r3}^G)$ is used as one of the most frequently used mutation operators. X_{best}^G is the best solution for the current generation. The difference vector's scaling is managed using the F control parameter. The crossover operator is then used to combine the target vector with its corresponding mutant vector, resulting in a trial vector (U_i^G).

$$u_{i,j}^G = \begin{cases} v_{i,j}^G, & if\ (rand\ <\ Cr\ or\ j = j_{rand}) \\ x_{i,j}^G, & otherwise \end{cases}. \tag{5}$$

Cr is the crossover rate and is between 0 and 1. Additionally, j_{rand} is a random integer in the range [1, D]. Selecting between the target vector (X_i^G) and its corresponding trial vector (U_i^G) determines whether the vector will be retained for the next generation. The selection procedure is as follows for minimising problems:

$$X_i^{G+1} = \begin{cases} U_i^G, & f\left(U_i^G\right) \le f\left(X_i^G\right) \\ X_i^G, & otherwise \end{cases}, \tag{6}$$

where $f(X_i^G)$ and $f(U_i^G)$ denote the objective functions of the target vector and the corresponding trial vector, respectively.

Table 1 contains data on the clustering of construction projects. The locations of construction projects are categorised in Table 1 into two clusters. Cluster 1 projects can be served by

Table 1: A numerical illustration of affected point clustering using the proposed DE-K-prototypes method.

Construction projects	Road slope	Weather conditions	The magnitude of the disaster	The density of the population	Risk on the road	Distance from depot1 (truck) Km	Distance from vehicle depot2 (truck) Km	Distance from airport (helicopter) Km	Width road (m)	Construction projects	Road slope	Weather conditions	The magnitude of the disaster	The density of the population	Risk on the road	Distance from depot1 (truck) Km	Distance from vehicle depot2 (truck) Km	Distance from airport (helicopter) Km	Width road (m)
1	low	Normal	Very high	2739	Low	8	5	0	12	**26**	Low	Good	High	6628	Low	1	8	13	8
2	low	Normal	Very high	3100	Low	12	8	11	8	**27**	Low	Good	High	1300	Low	2	9	14	8
3	low	Normal	High	2050	Low	10	5	10	8	**28**	Low	Good	High	1400	Low	3	9	15	8
4	low	Good	High	450	Low	8	5	1	12	**29**	Low	Good	Medium	1500	Medium	5	10	17	8
5	low	Good	Very high	850	Low	9	5	3	12	**30**	Medium	Normal	Medium	700	Medium	7	11	18	8
6	low	Good	High	1416	Low	3	10	13	12	**31**	Low	Normal	Medium	600	Medium	7	10	17	8
7	Medium	Good	Medium	1200	Medium	5	13	16	8	**32**	Low	Normal	High	3000	Medium	1	7	12	8
8	Medium	Normal	Medium	1020	Medium	6	14	17	8	**33**	Low	Good	High	4000	Medium	6	5	10	8
9	High	Bad	Medium	1201	Medium	7	14	19	8	**34**	Low	Good	Medium	300	Medium	7	3	8	8
10	High	Bad	High	500	Medium	8	15	20	8	**35**	Low	Good	High	1400	Medium	8	3	8	8
11	High	Normal	Very high	900	Medium	67	70	75	12	**36**	Low	Good	High	1500	Medium	8	2	7	8
12	High	Bad	Very high	1316	Medium	65	72	77	12	**37**	Low	Good	High	3500	Medium	8	3	8	8
13	High	Bad	Very high	800	Medium	68	71	77	8	**38**	Medium	Normal	High	2000	Medium	9	3	8	8
14	Medium	Normal	High	500	Medium	8	13	18	8	**39**	Low	Normal	High	1000	Medium	7	2	7	8
15	Medium	Good	High	351	Medium	9	15	20	8	**40**	Low	Normal	Medium	1000	Medium	7	2	7	8
16	Medium	Good	High	450	Medium	9	11	16	8	**41**	Low	Normal	High	4000	Medium	8	7	12	8
17	Medium	Normal	High	500	Medium	18	16	13	12	**42**	High	Bad	Medium	50	Medium	18	4	13	8
18	low	Normal	High	7703	Medium	25	4	15	8	**43**	Low	Normal	High	1320	Medium	8	3	8	8
19	High	Bad	Very high	2584	High	75	70	65	8	**44**	Medium	Normal	High	450	Medium	8	5	8	8
20	High	Bad	Very high	204	High	87	82	78	8	**45**	Medium	Bad	Very high	700	High	13	8	13	8
21	High	Bad	Very high	1202	High	81	76	71	8	**46**	Medium	Bad	Very high	1500	High	7	5	10	8
22	High	Bad	Very high	202	High	80	75	70	8	**47**	Low	Good	High	500	Medium	7	4	9	8
23	High	Bad	Very high	302	High	75	70	65	8	**48**	Low	Good	Very high	500	Medium	8	4	12	8
24	High	Bad	Very high	1500	High	85	80	75	8	**49**	Medium	Normal	Medium	500	Medium	8	4	13	8
25	Medium	Good	High	1500	Medium	4	12	17	8	**50**	Low	Normal	High	600	Medium	8	14	16	8

Algorithm 1: *DE-K-Prototypes algorithm*

Randomly generate N solutions;
Initialization of iteration $\zeta = 1$;
while generation $\zeta \leq \zeta_{max}$
  Generating the mutant vectors using Equation 4;
  Generating trial vectors using Equation 5;
  Evaluate the objective values of the newly generated solutions using Equation 1;
  Generate the population for the next generation by selecting the best trial vectors;
  $\zeta = \zeta + 1$
end

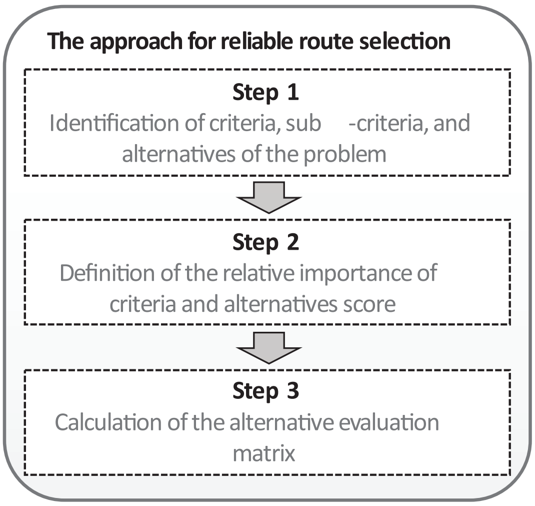

Figure 2: The steps of selecting the reliable routes.

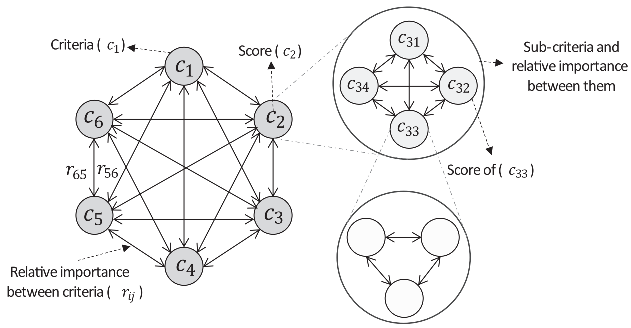

Figure 3: Criteria and subcriteria framework adopted from Baykasoglu (2014).

Table 2: The scores of alternatives.

Qualitative measure	Crisp score
Exceptionally low	0
Extremely low	1
Very low	2
Low	3
Below average	4
Average	5
Above average	6
High	7
Very high	8
Extremely high	9
Exceptionally high	10

both land vehicles and aerial vehicles. While cluster 2 projects include locations that are inaccessible via land and should be served by air vehicles.

3.2 Reliable route selection

In this section, the obtained clusters are prioritised according to factors affecting route reliability in order to determine the most reliable route for distributing construction materials. The type of road (autobahn or highway), the degree of mountainous areas, and geographical characteristics all affect the reliability of cluster 1, which are accessible through the ground and aerial vehicles. Cluster 2's reliability is affected by the magnitude of the disaster, the regional context (urban or rural), the weather conditions, the region's demand, and the distance between the air vehicle depot and the location of construction projects. The approach is presented in Fig. 2.

The graph and its dependencies are used to represent the identification of the influencing factor on the process by conducting an expert survey or using data from the literature (Geetha & Sekar, 2016). There are nodes and directed edges that make up the graph, as depicted in Fig. 3. Each node $\mathfrak{n}_i$ represents the i-th criterion for alternative selection, while the edges represent the relative importance of the criteria, with the same number of nodes and alternatives. A directed edge is drawn from i to j ($\mathfrak{c}_{ij}$) and vice versa, if node i is more important than node j in alternative selection (Rao & Padmanabhan, 2007).

The relative importance of criteria and alternative scores are defined following the first step. If the criterion is qualitative, the values of the alternatives score can be derived using a zero-to-one rating scale (Nasiri & ShisheGar, 2014), as seen in Table 2.

Normalization is necessary when employing quantitative criteria. Thus, if $\mathfrak{v}_i$ and $\mathfrak{v}_j$ are criteria values of alternative i and j, respectively, $\frac{\mathfrak{v}_i}{\mathfrak{v}_j}$ should be normalised (Mohaghar *et al.*, 2013). Following the calculation of all the criteria values ($i = 1, \ldots, N$) for an alternative, we create a criteria rating matrix for that alternative.

$$[\psi] = \begin{bmatrix} \mathcal{C}_{11} & 0 & \ldots & 0 \\ 0 & \mathcal{C}_{22} & \ldots & 0 \\ \ldots & \ldots & \ldots & \ldots \\ 0 & 0 & \ldots & \mathcal{C}_{nn} \end{bmatrix}. \quad (7)$$

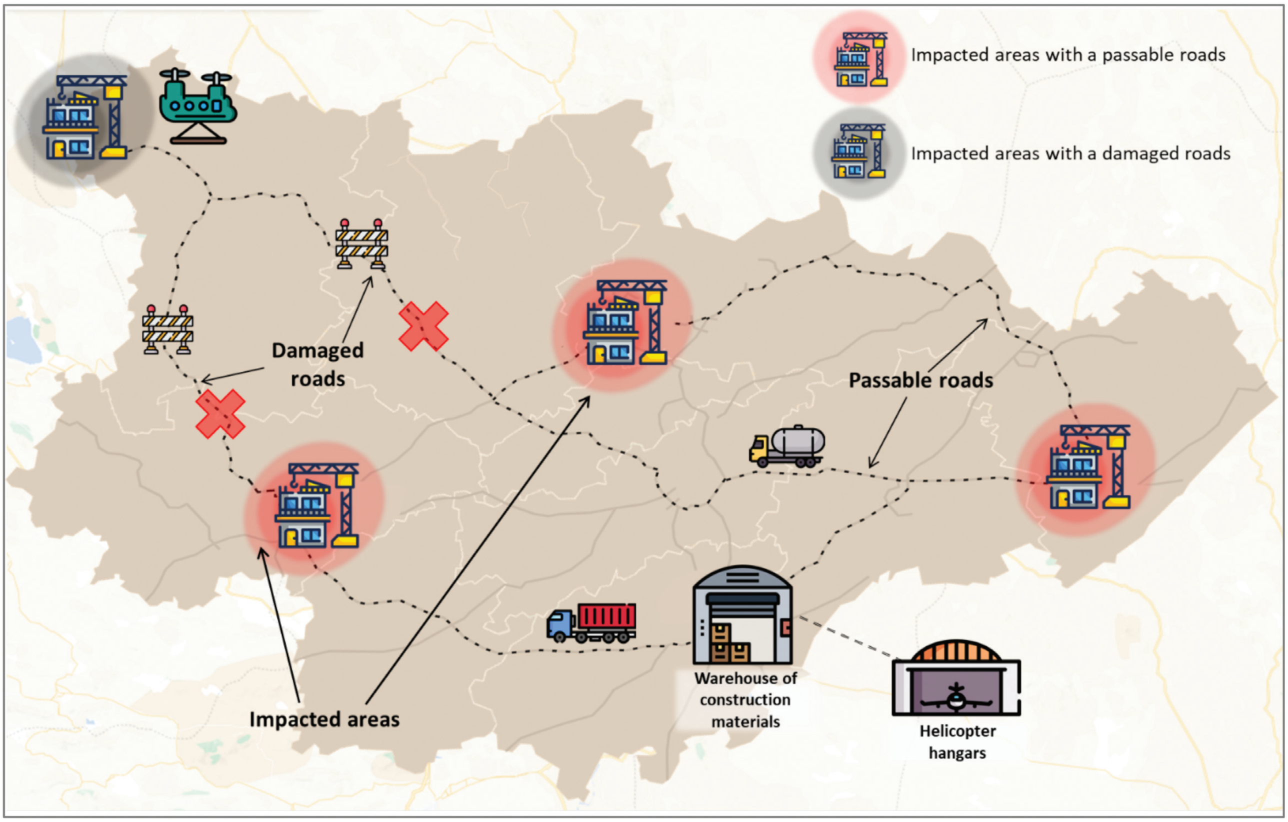

Figure 4. An illustration of the problem in schematic form.

However, the relative importance of criteria ($\mathfrak{r}_{ij}$) can range between zero and one. The relationship between $\mathfrak{r}_{ij}$ and $\mathfrak{r}_{ji}$ does not have to be compensatory. As shown in Table 3, it can be $\mathfrak{r}_{ji} = \frac{1}{\mathfrak{r}_{ij}}$.

After this step, the relative importance matrix is defined as follows:

$$[\beta] = \begin{bmatrix} 0 & \mathfrak{r}_{12} & \dots & \mathfrak{r}_{in} \\ \mathfrak{r}_{21} & 0 & \dots & \mathfrak{r}_{2n} \\ \dots & \dots & \dots & \dots \\ \mathfrak{r}_{n1} & \dots & \dots & 0 \end{bmatrix}. \tag{8}$$

Following the identification of β and ψ, the alternative evaluation matrix ξ is obtained as follows:

$$\xi = \psi + \beta = \begin{bmatrix} \mathcal{C}_1 & \mathfrak{r}_{12} & \mathfrak{r}_{13} & \dots & \mathfrak{r}_{1n} \\ \mathfrak{r}_{21} & \mathcal{C}_2 & \mathfrak{r}_{23} & \dots & \mathfrak{r}_{2n} \\ \mathfrak{r}_{31} & \mathfrak{r}_{32} & \mathcal{C}_3 & \dots & \mathfrak{r}_{3n} \\ \dots & \dots & \dots & \dots & \dots \\ \mathfrak{r}_{n1} & \mathfrak{r}_{n2} & \mathfrak{r}_{n3} & \dots & \mathcal{C}_{in} \end{bmatrix}. \tag{9}$$

The permanent of matrix ξ, *per*(ξ) provides the rating for the alternative. For every alternative *per*(ξ) should be calculated and arranged in a descending order (Nasiri & ShisheGar, 2014). The alternative with the highest *per*(ξ) value is more preferable. Below is the equation that represents the permanent value calculation function (Nasiri & ShisheGar, 2014).

$$\begin{aligned} \mathrm{Per}(\xi) = {} & \prod_{i=1}^{\mathcal{N}} \mathcal{C}_i + \sum_{i,j,\dots,\mathcal{N}} (\mathfrak{r}_{ij}.\mathfrak{r}_{ji}).\mathcal{C}_{\mathfrak{k}}.\mathcal{C}_{\mathfrak{l}}\dots\mathcal{C}_{\mathcal{N}} \\ & + \sum_{i,j,\dots,\mathcal{N}} (\mathfrak{r}_{ij}.\mathfrak{r}_{j\mathfrak{k}}.\mathfrak{r}_{\mathfrak{k}i} + \mathfrak{r}_{i\mathfrak{k}}.\mathfrak{r}_{\mathfrak{k}j}.\mathfrak{r}_{ji}).\mathcal{C}_{\mathfrak{l}}.\mathcal{C}_{n}\dots\mathcal{C}_{\mathcal{N}} \\ & + \left\{ \sum_{i,j,\dots,\mathcal{N}} (\mathfrak{r}_{ij}.\mathfrak{r}_{ji})(\mathfrak{r}_{\mathfrak{k}\mathfrak{l}}.\mathfrak{r}_{\mathfrak{l}\mathfrak{k}}).\mathcal{C}_{n}.\mathcal{C}_{m}\dots.\mathcal{C}_{\mathcal{N}} \right. \\ & \left. + \sum_{i,j,\dots,\mathcal{N}} (\mathfrak{r}_{ij}.\mathfrak{r}_{\mathfrak{k}j}.\mathfrak{r}_{\mathfrak{k}\ell}.\mathfrak{r}_{\ell i} + \mathfrak{r}_{i\ell}.\mathfrak{r}_{\ell\mathfrak{k}}.\mathfrak{r}_{\mathfrak{k}j}.\mathfrak{r}_{ji}).\mathcal{C}_{n}.\mathcal{C}_{m}\dots\mathcal{C}_{\mathcal{N}} \right\} \\ & + \left\{ \sum_{i,j,\dots,\mathcal{N}} (\mathfrak{r}_{ij}.\mathfrak{r}_{ji})(\mathfrak{r}_{\mathfrak{k}\ell}.\mathfrak{k}_{\ell n}.\mathfrak{r}_{n\mathfrak{k}}).\mathcal{C}_{m}.\mathcal{C}_{o}\dots\mathcal{C}_{\mathcal{N}} \right. \\ & + \sum_{i,j,\dots,\mathcal{N}} (\mathfrak{r}_{ij}.\mathfrak{r}_{j\mathfrak{k}}.\mathfrak{r}_{\mathfrak{k}\ell}.\mathfrak{r}_{\ell n}.\mathfrak{r}_{ni} \\ & \left. + \mathfrak{r}_{in}.\mathfrak{r}_{n\ell}.\mathfrak{r}_{\ell\mathfrak{k}}.\mathfrak{r}_{\mathfrak{k}j}.\mathfrak{r}_{ji}).\mathcal{C}_{m}.\mathcal{C}_{o}\dots\mathcal{C}_{\mathcal{N}} \right\} + \cdots \end{aligned} \tag{10}$$

3.3 Modelling and the proposed solving method

There is a specific number of post-disaster reconstruction projects in areas that have been impacted by a destructive disaster. Each project needs $\tilde{\mathcal{Q}}_{imp}$ construction material type $\mathfrak{m}$ in the time period $\mathfrak{p}$. Materials should be provided for construction projects from a number of warehouses. For distributing materials from warehouses to construction sites, two different types

Table 3: The relative importance of criteria.

Definition of the class	$\mathfrak{r}_{ij}$	$\mathfrak{r}_{ij} = 1 - \mathfrak{r}_{ij}$
Two criteria are equally important	0.5	0.5
One criterion is slightly more important than others	0.6	0.4
One criterion is more important than others	0.7	0.3
One criterion is very important than others	0.8	0.2
One criterion is exceptionally important than others	0.9	0.1
One criterion is the most important, other not important	1.0	0.0

of vehicles, including land and aerial vehicles, are used, and the number of each type is limited to $\mathcal{N}_{\mathfrak{v}}$ and $\mathcal{N}_{\mathfrak{h}}$ vehicles. All vehicles are available from the beginning of the transportation. Each vehicle can carry a limited amount of materials. The construction projects are located in two different areas; some of them are accessible through the roads, while other projects are in areas that are not accessible using the roads; therefore, aerial vehicles should be used to provide the required material for them. Vehicles move in a network represented by a graph in which nodes are locations of construction projects and depots and arcs are the routes between each pair of nodes. However, due to the impact of the disaster on the road network, travel times on network links vary depending on time, so $\mathfrak{t}_{\mathfrak{v}ij\mathfrak{p}}$ denotes the travel time for vehicle type $\mathfrak{v}$ from node i to j in the time period $\mathfrak{p}$. To reach a comprehensive plan, we consider three objectives in this model, minimising the total travel time, maximising the reliability of the route, and minimising the total weighted undelivered materials to projects. See Fig. 4. For the schematic presentation of the problem.

Real-world decision-making problems can be reduced to their essential elements by employing mathematical modelling techniques. If all the details are included in a model, it may be impossible to model real-world problems. The most useful models rely on assumptions that preserve the system's fundamental properties while also simplifying it. Keeping models manageable and accurate in light of this fact necessitates simplifying assumptions. Mathematical models that incorporate these assumptions are highly effective, as evidenced by the following:

(i) The number of vehicles is finite, and different types of vehicles are used to deliver materials to the projects. As a result, the transport fleet of vehicles is heterogeneous, and their capacity and speed are different.
(ii) The origin of all vehicles is known in advance.
(iii) The vehicle's capacity is more than the demand so that there is no interruption in service.
(iv) The place of distribution of material and warehouses of vehicles is the same, and the place and number of warehouses are predetermined.
(v) Available construction material is sufficient to respond to the projects.
(vi) Distribution operations are performed for several types of construction materials.
(vii) The location of each project is known, and their distance from the warehouse is known.
(viii) Each rescue vehicle returns to the starting point of the movement (warehouse) after the end of the operation (closed route).
(ix) The distribution of construction materials is performed from several warehouses, where the warehouses for vehicles and the warehouses for storing construction materials are the same.
(x) The construction projects are located in two clusters, and all those points are prioritized based on the factors affecting reliability.
(xi) A damaged vehicle cannot be repaired at an acceptable time to be able to continue its work.
(xii) If the product in a particular scenario, before the car breakdown, has reached the location of construction projects, the service is complete, and shortage does not occur.
(xiii) After a vehicle breakdown, other vehicles should not perform their service duties and should act according to their own schedule.
(xiv) The demand for each project might not be fully met and may be in short supply.
(xv) Construction materials are distributed over different periods.

3.3.1 The mathematical model

The variables and parameters listed below are used in the development of the mathematical model.

Notations, sets, and parameters

$\mathfrak{v} \in \mathcal{N}_{\mathfrak{v}}$	Set of trucks
$\mathfrak{h} \in \mathcal{N}_{\mathfrak{h}}$	Set of helicopters
$\mathfrak{a} \in \mathcal{N}_{\mathfrak{a}}$	Set of the location of projects with a passable access road
$\mathfrak{a}' \in \mathcal{N}_{\mathfrak{a}'}$	Set of the location of projects with a damaged access road
$\mathcal{N}_{\mathfrak{a}} \cup \mathcal{N}_{\mathfrak{a}'} \subseteq \mathcal{N}_{\hat{\mathfrak{a}}}$	
$i, j \in \mathcal{I}, \mathcal{J}$	Set of all locations, including depots
$\mathfrak{m} \in \mathcal{M}$	Set of construction material types
$\mathfrak{p} \in \mathcal{P}$	Set of time periods
$\mathfrak{s} \in \mathcal{S}$	Set of time scenarios
$\mathcal{C}_{\mathfrak{v}}$	The capacity of vehicle $\mathfrak{v} \in \mathcal{N}_{\mathfrak{v}} \cup \mathcal{N}_{\mathfrak{h}}$
$\tilde{\mathcal{Q}}_{i\mathfrak{m}\mathfrak{p}}$	The demand of project i for construction material type $\mathfrak{m}$ in time period $\mathfrak{p}$
$\omega_{i\mathfrak{m}\mathfrak{p}}$	The value of construction material type $\mathfrak{m}$ in time period $\mathfrak{p}$ for the project i
$\mathfrak{r}_{ij}$	The permanent value of node i to j based on the reliability index
$\mathcal{T}_{j\mathfrak{v}\mathfrak{p}}$	Arrival time of vehicle $\mathfrak{v}$ to node i in time period $\mathfrak{p}$
$\delta^{\mathfrak{s}}_{\mathfrak{v}\mathfrak{p}}$	Break down scenario for vehicle $\mathfrak{v}$, it means $\mathfrak{v}$ in scenario $\mathfrak{s}$ fails after δ unit time in time period $\mathfrak{p}$
$\mathfrak{d}_{\mathfrak{v}}$	The location of depot vehicle $\mathfrak{v} \in (\mathcal{N}_{\mathfrak{v}} \cup \mathcal{N}_{\mathfrak{h}})$
$\xi_{\mathfrak{p}}$	Start time of the period $\mathfrak{p}$
$\mathfrak{t}_{\mathfrak{v}ij\mathfrak{p}}$	Travel time for vehicle type $\mathfrak{v}$ from node i to j in time period $\mathfrak{p}$

Decision variables

$$\mathfrak{x}_{\mathfrak{v}\mathfrak{i}\mathfrak{j}\mathfrak{p}} = \begin{cases} 1 & \text{if vehicle } \mathfrak{v} \text{ travel from node } \mathfrak{i} \text{ to node } \mathfrak{j} \text{ in time period } \mathfrak{p} \\ 0 & \text{otherwise} \end{cases}$$

$$\mathfrak{y}^{\mathfrak{s}}_{\mathfrak{i}\mathfrak{p}} = \begin{cases} 1 & \text{if the material is not delivered to the project } \mathfrak{i} \text{ in } \textit{time period } \mathfrak{p} \text{ under scenario } \mathfrak{s} \\ 0 & \text{otherwise} \end{cases}$$

Model formulation

Mathematically, the proposed model can be expressed as follows:

$$\mathcal{M}in \sum_{\mathfrak{i}\in\mathcal{I}}\sum_{\mathfrak{j}\in\mathcal{J}}\sum_{\mathfrak{v}\in\mathcal{V}}\sum_{\mathfrak{p}\in\mathcal{P}} \mathfrak{t}_{\mathfrak{v}\mathfrak{i}\mathfrak{j}\mathfrak{p}}\mathfrak{x}_{\mathfrak{v}\mathfrak{i}\mathfrak{j}\mathfrak{p}},$$

$$\mathcal{M}a\mathfrak{x} \sum_{\mathfrak{i}\in\mathcal{I}}\sum_{\mathfrak{j}\in\mathcal{J}}\sum_{\mathfrak{v}\in\mathcal{V}}\sum_{\mathfrak{p}\in\mathcal{P}} \mathfrak{r}_{\mathfrak{i}\mathfrak{j}}\mathfrak{x}_{\mathfrak{v}\mathfrak{i}\mathfrak{j}\mathfrak{p}}, \tag{11}$$

$$\mathcal{M}in \sum_{\mathfrak{s}\in\mathcal{S}}\sum_{\mathfrak{p}\in\mathcal{P}}\sum_{\mathfrak{m}\in\mathcal{M}}\sum_{\mathfrak{i}\in\mathcal{N}_{\hat{\mathfrak{a}}}} \mathfrak{y}^{\mathfrak{s}}_{\mathfrak{i}\mathfrak{p}}\tilde{\mathcal{Q}}_{\mathfrak{i}\mathfrak{m}\mathfrak{p}}\omega_{\mathfrak{i}\mathfrak{m}\mathfrak{p}},$$

s.to.

$$\sum_{\mathfrak{i}\in\mathcal{N}_{\mathfrak{a}}\cup\mathfrak{d}_{\mathfrak{v}}} \mathfrak{x}_{\mathfrak{v}\mathfrak{i}\mathfrak{j}\mathfrak{p}} = \sum_{\mathfrak{i}\in\mathcal{N}_{\mathfrak{a}}\cup\mathfrak{d}_{\mathfrak{v}}} \mathfrak{x}_{\mathfrak{v}\mathfrak{j}\mathfrak{i}\mathfrak{p}} \quad \forall \mathfrak{j}\in\mathcal{N}_{\mathfrak{a}}, \mathfrak{v}\in\mathcal{N}_{\mathfrak{v}}, \mathfrak{p}\in\mathcal{P} \tag{12}$$

$$\sum_{\mathfrak{i}\in\mathcal{N}_{\hat{\mathfrak{a}}}\cup\mathfrak{d}_{\mathfrak{h}}} \mathfrak{x}_{\mathfrak{h}\mathfrak{i}\mathfrak{j}\mathfrak{p}} = \sum_{\mathfrak{i}\in\mathcal{N}_{\hat{\mathfrak{a}}}\cup\mathfrak{d}_{\mathfrak{h}}} \mathfrak{x}_{\mathfrak{h}\mathfrak{j}\mathfrak{i}\mathfrak{p}} \quad \forall\, \mathfrak{j}\in\mathcal{N}_{\hat{\mathfrak{a}}}, \mathfrak{h}\in\mathcal{N}_{\mathfrak{h}}, \mathfrak{p}\in\mathcal{P} \tag{13}$$

$$\sum_{\mathfrak{i}\in\mathfrak{d}_{\mathfrak{v}}}\sum_{\mathfrak{j}\in\mathcal{N}_{\hat{\mathfrak{a}}}} \mathfrak{x}_{\mathfrak{v}\mathfrak{i}\mathfrak{j}\mathfrak{p}} = 1 \quad \forall\, \mathfrak{v}\in\mathcal{N}_{\mathfrak{v}}\cup\mathcal{N}_{\mathfrak{h}}, \mathfrak{p}\in\mathcal{P} \tag{14}$$

$$\sum_{\mathfrak{i}\in\mathcal{N}_{\hat{\mathfrak{a}}}}\sum_{\mathfrak{j}\in\mathfrak{d}_{\mathfrak{v}}} \mathfrak{x}_{\mathfrak{v}\mathfrak{i}\mathfrak{j}\mathfrak{p}} = 1 \quad \forall\, \mathfrak{v}\in\mathcal{N}_{\mathfrak{v}}\cup\mathcal{N}_{\mathfrak{h}}, \mathfrak{p}\in\mathcal{P} \tag{15}$$

$$\sum_{\mathfrak{i}\in\mathfrak{d}_{\mathfrak{v}}}\sum_{\mathfrak{j}\in\mathcal{N}_{\mathfrak{a}'}} \mathfrak{x}_{\mathfrak{v}\mathfrak{i}\mathfrak{j}\mathfrak{p}} + \sum_{\mathfrak{i}\in\mathcal{N}_{\mathfrak{a}'}}\sum_{\mathfrak{j}\in\mathfrak{d}_{\mathfrak{v}}} \mathfrak{x}_{\mathfrak{v}\mathfrak{i}\mathfrak{j}\mathfrak{p}} = 0 \quad \forall\, \mathfrak{v}\in\mathcal{N}_{\mathfrak{v}}, \mathfrak{p}\in\mathcal{P} \tag{16}$$

$$\sum_{\mathfrak{i}\in\mathfrak{d}_{\mathfrak{v}}}\sum_{\mathfrak{j}\in\mathcal{N}_{\hat{\mathfrak{a}}}} \mathfrak{x}_{\mathfrak{v}\mathfrak{i}\mathfrak{j}\mathfrak{p}}\tilde{\mathcal{Q}}_{\mathfrak{i}\mathfrak{m}\mathfrak{p}} \le \mathcal{C}_{\mathfrak{v}} \quad \forall\, \mathfrak{v}\in\mathcal{N}_{\mathfrak{v}}\cup\mathcal{N}_{\mathfrak{h}}, \mathfrak{p}\in\mathcal{P} \tag{17}$$

$$\mathcal{T}_{\mathfrak{j}\mathfrak{v}\mathfrak{p}} = \sum_{\mathfrak{i}\in\mathfrak{d}_{\mathfrak{v}}} \mathfrak{t}_{\mathfrak{v}\mathfrak{i}\mathfrak{j}\mathfrak{p}}\mathfrak{x}_{\mathfrak{v}\mathfrak{i}\mathfrak{j}\mathfrak{p}} + \xi_{\mathfrak{p}} \quad \forall \mathfrak{j}\in\mathcal{N}_{\hat{\mathfrak{a}}}, \mathfrak{v}\in\mathcal{N}_{\mathfrak{v}}\cup\mathcal{N}_{\mathfrak{h}}, \mathfrak{p}\in\mathcal{P} \tag{18}$$

$$\mathcal{M}\left(1-\mathfrak{y}^{\mathfrak{s}}_{\mathfrak{i}\mathfrak{p}}\right) \ge \left(\mathcal{T}_{\mathfrak{i}\mathfrak{v}\mathfrak{p}} - \delta^{\mathfrak{s}}_{\mathfrak{v}\mathfrak{p}}\right) \quad \forall \mathfrak{i}\in\mathcal{N}_{\hat{\mathfrak{a}}}, \mathfrak{s}\in\mathcal{S}, \mathfrak{v}\in\mathcal{N}_{\mathfrak{v}}\cup\mathcal{N}_{\mathfrak{h}}, \mathfrak{p}\in\mathcal{P} \tag{19}$$

$$\mathfrak{x}_{\mathfrak{v}\mathfrak{i}\mathfrak{j}\mathfrak{p}} \in \{0, 1\} \quad \forall \mathfrak{v}, \mathfrak{i}, \mathfrak{j}, \mathfrak{p} \tag{20}$$

$$\mathcal{T}_{\mathfrak{i}\mathfrak{v}\mathfrak{p}} \ge 0 \quad \forall \mathfrak{v}, \mathfrak{i}, \mathfrak{p} \tag{21}$$

$$\mathfrak{y}^{\mathfrak{s}}_{\mathfrak{i}\mathfrak{p}} \in \{0, 1\} \quad \forall \mathfrak{i}, \mathfrak{p}, \mathfrak{s}. \tag{22}$$

The first objective function minimises the total travel time, the second objective function maximises the reliability of routes, and the third objective function minimises the total weighted undelivered materials to projects. Constraint (2) ensures that each truck leaves a project after entering and servicing it. Constraint (3) ensures that each helicopter leaves a project after entering and servicing it. Constraints (4) and (5) ensure that after servicing any nodes, all vehicles (i.e. truck and helicopter) must return to the start point, successfully closing the route. Constraint (6) asserts that trucks cannot serve projects with impassable roads. Constraints (7) refer to the vehicle capacity limitations. Constraint (8) calculates the vehicle's arrival time at construction sites. Constraint (9) indicates whether or not the shortage exists in the given scenarios. Constraints (10) to (12) define the type of the variables.

Pareto-optimal or non-dominated solutions are explored in multi-objective problems rather than single optimal solutions. If a solution cannot be improved in one objective function without degrading its performance in at least one other objective, it is Pareto optimal (Mavrotas, 2009). As a result of these Pareto optimal solutions, the Pareto front of the problem is constructed, from which decision makers can choose the final preferred compromise solution. Several methods for multi-objective problems have been proposed in the literature. In this study, the augmented ε-constraint method (AUGMECON), similar to Esmaili *et al.* (2011), transforms the multi-objective problem into a single-objective problem.

Due to the uncertainty in a disaster situation and becoming closer to reality, the received demand for construction projects is fuzzy numbers in the proposed model. A symmetrical triangle distribution is considered for indicating the fuzzy parameter due to its applicability and ease of calculation. Because of its high efficiency, the Jimenez method is used to transform the current model into its corresponding deterministic model (Jiménez *et al.*, 2007). The following equations represent changes in the objective function and constraints:

$$\mathcal{M}in \sum_{\mathfrak{i}\in\mathcal{I}}\sum_{\mathfrak{j}\in\mathcal{J}}\sum_{\mathfrak{v}\in\mathcal{V}}\sum_{\mathfrak{p}\in\mathcal{P}} \mathfrak{t}_{\mathfrak{v}\mathfrak{i}\mathfrak{j}\mathfrak{p}}\mathfrak{x}_{\mathfrak{v}\mathfrak{i}\mathfrak{j}\mathfrak{p}},$$

$$\mathcal{M}a\mathfrak{x} \sum_{\mathfrak{i}\in\mathcal{I}}\sum_{\mathfrak{j}\in\mathcal{J}}\sum_{\mathfrak{v}\in\mathcal{V}}\sum_{\mathfrak{p}\in\mathcal{P}} \mathfrak{r}_{\mathfrak{i}\mathfrak{j}}\mathfrak{x}_{\mathfrak{v}\mathfrak{i}\mathfrak{j}\mathfrak{p}}, \tag{23}$$

$$\mathcal{M}in \sum_{\mathfrak{s}\in\mathcal{S}}\sum_{\mathfrak{p}\in\mathcal{P}}\sum_{\mathfrak{m}\in\mathcal{M}}\sum_{\mathfrak{i}\in\mathcal{N}_{\hat{\mathfrak{a}}}} \mathfrak{y}^{\mathfrak{s}}_{\mathfrak{i}\mathfrak{p}}\left(\frac{\mathcal{Q}^1_{\mathfrak{i}\mathfrak{m}\mathfrak{p}}+\mathcal{Q}^2_{\mathfrak{i}\mathfrak{m}\mathfrak{p}}+\mathcal{Q}^3_{\mathfrak{i}\mathfrak{m}\mathfrak{p}}}{4}\right)\omega_{\mathfrak{i}\mathfrak{m}\mathfrak{p}},$$

Subject to :

Other constraints in the model. (24)

$$\sum_{\mathfrak{i}\in\mathfrak{d}_{\mathfrak{v}}}\sum_{\mathfrak{j}\in\mathcal{N}_{\hat{\mathfrak{a}}}} \mathfrak{x}_{\mathfrak{v}\mathfrak{i}\mathfrak{j}\mathfrak{p}}\left[a.\left(\frac{\mathcal{Q}^1_{\mathfrak{i}\mathfrak{m}\mathfrak{p}}+\mathcal{Q}^2_{\mathfrak{i}\mathfrak{m}\mathfrak{p}}}{2}\right)\right. \tag{25}$$

$$\left. +\left(1-a\right)\left(\frac{\mathcal{Q}^2_{\mathfrak{i}\mathfrak{m}\mathfrak{p}}+\mathcal{Q}^3_{\mathfrak{i}\mathfrak{m}\mathfrak{p}}}{2}\right)\right] \le \mathcal{C}_{\mathfrak{v}} \quad \forall\, \mathfrak{v}\in\mathcal{N}_{\mathfrak{v}}\cup\mathcal{N}_{\mathfrak{h}}, \mathfrak{p}\in\mathcal{P}.$$

4. Multi-Objective Meta-heuristics Algorithms

When a problem has multiple objectives, it is difficult to find the best solution (Tirkolaee *et al.*, 2022; Yuan *et al.*, 2022). Many real-world optimisation problems are made more difficult by the presence of multiple objectives (Pasha *et al.*, 2022). Meta-heuristic algorithms can be used to solve these problems (Fathollahi-Fard *et al.*, 2021b). Meta-heuristic algorithms have some advantages (Dulebenets, 2021). Any problem that can be expressed as a function-optimisation problem can be solved with these methods (Fathollahi-Fard *et al.*, 2021b); these methods tend to be more straightforward to understand and implement (Theophilus *et al.*, 2021), and they can handle more complex problems with ease (Pasha *et al.*, 2020). In this study, two widely used multi-objective meta-heuristic algorithms, NSGA-II and MOEA/D, are used to solve the problem. The pseudocode and algorithm properties are discussed in the following section.

4.1 NSGA-II

NSGA-II, which was introduced for the first time by Deb *et al.* (2002), is one of the most widely applicable and well-proposed genetic algorithm (GA)-based algorithms for solving multi-objective optimisation problems. NSGA-II begins by randomly generating a population of size A_{ξ} (Babaeinesami *et al.*, 2022). The objective values of a population are evaluated using an objective function. The population is then ranked according to the non-domination sorting procedure in order to generate Pareto fronts. Each individual in the population under consideration is assigned a rank equal to its non-domination level, with the first front containing individuals with the lowest rank, the second front containing individuals with the second rank, and so on (Tirkolaee *et al.*, 2020b). The following step calculates the crowding distance between members on each front using a linear distance criterion. Due to the fact that a binary tournament selection operator based on a crowded-comparison operator is used, both the rank and crowding distance of each member of the population must be calculated. Two members of the population are initially selected using this selection operator. The member with the greater crowding distance is then chosen if their ranks are equal. Otherwise, the lower ranking member is chosen. Following that, a new population of offspring with a size of n is created using the selection, crossover, and mutation operators to create a population composed of the current population and the new population of size ($A_\xi + n$). In this study, one point crossover has been used. Finally, using the sorting procedure, a population with the exact size of A_ξ is obtained. The solutions are sorted twice in this procedure: first by their crowding distances in descending order, and then by their ranks in ascending order (Tirkolaee *et al.*, 2019). By repeating the preceding steps in order, the new population is used to generate the next generation of offspring. This procedure is repeated until the termination condition is satisfied. After implementing NSGA-II, a set of non-dominated Pareto-optimal solutions is obtained, as all solutions are optimal in terms of multi-objective optimisation. Algorithm 2 presents the pseudocode of NSGA-II.

4.2 MOEA/D

The MOEA/D algorithm for the multi-objective problems is introduced by Zhang and Li (2007). MOEA/D uses a set of uniformly distributed weight vectors $W = \{w^1, \ldots, w^\mu\}$ to decompose a multi-objective optimisation problem with M objectives into single-objective subproblems. At the start of the search, all members of the population are generated randomly in the search space S. An index list $B^i = \{i_1, \ldots, i_T\}$ is initialised for each subproblem index $i \in \{1, \ldots, \mu\}$, which is used for mating and replacement selections: B^i is composed of the indices of the T weight vectors that are closest to w^i in the weight vector space, where T denotes the neighbourhood size (Fathollahi-Fard *et al.*, 2021a). Following initialisation, the following steps are repeated for each subproblem $i \in \{1, \ldots, \mu\}$ until the search criteria for termination are met. The parent indices k and l are randomly chosen from B^i for each i. Then, by combining x^k and x^l, a child u^i is generated. If necessary, a mutation opera-tor is applied to the child u^i. After generating u^i, a pre-defined scalarising function g is used to perform the replacement selection. On the basis of g, the individual x^j is compared to the child u^i for each $j \in B^i$. If u^i is superior to x^j in terms of their weight vector w^j scalarising function values, x^j is replaced by u^i.

Since the replacement of individuals is based on their scalarising function values, g plays a crucial role in MOEA/D. Although there are a number of scalarising functions as reviewed in (Pescador-Rojas *et al.*, 2017), in this paper, we follow the approach of (Wang *et al.*, 2015).

4.3 Solution representation

The solution representation should be simple to decode in order to minimise the algorithm's computational cost. As a result, the solution representation illustrated in Fig. 5 is used in this study. A cube is considered in this type of answer representation, with the dimensions of the solution being construction projects (J), vehicles (V), and time period (t). In the solution depicted in Fig. 5, five construction projects, three vehicles, and three periods are assumed. Each cell in this solution representation is filled with a value between 0 and 1.

To determine how vehicles are used to service construction projects during each period, the maximum number in each column and row is determined and marked. The columns' maximum values are indicated in blue, while the rows' maximum values are indicated in red. According to the priority winch established in the previous step, in each period, construction projects are assigned to a different vehicle, and the sequence of visits to each project by a particular vehicle is determined by the cell values. For instance, in the first period, vehicle one goes to project 5, and then goes to project 3.

Figure 6 shows the answer for each of the three periods separately. During the first period, vehicle 1 is assigned to projects 3 and 5, vehicle 2 is assigned to project 2, and vehicle 3 is assigned to projects 1 and 4. Then we find that the construction materials are distributed in the following order: Vehicle 1 is routed to project 5 first, then to project 3. Vehicle 2 only serves project 2, while vehicle 3 first serves project 4 and then project 1. Vehicle 1 is assigned to projects 3 and 5, vehicle 2 is assigned to project 4, and vehicle 3 is assigned to projects 1 and 2. Then we find that the construction materials are distributed in the following order: Vehicle 1 goes to project 5 and then to project 3. Vehicle 2 only serves project 4, whereas vehicle 3 first serves project 2 and then project 1. During the third period, vehicle 1 is assigned to projects 2 and 3, vehicle 2 is assigned to project 4, and vehicle 3 is assigned to projects 1 and 5. Then we see that the construction materials are distributed in the following order: Vehicle 1 goes to project 2 and then to project 3. Vehicle 2 only serves project 4, while vehicle 3 first serves project 5 and then project 1.

5. Computational Results

This section discusses the model proposed and the proposed solution approach for improving the distribution of post-disaster construction supplies after a large-scale disaster. First, in Section 5.1, the performance of the model and proposed algorithms for small-size problems are evaluated. The study's algorithms were implemented in *MATLAB 2018b*, and the mathematical model was coded in *GAMS* 25.0.2 and solved using the *CPLEX* solver on *an Intel Core i7 @ 2.5 GHz PC* with 8 GB of RAM running Microsoft Windows 10. Section 5.2 explains the evaluating metrics and the procedure for generating the instances of the problem. Section 5.3 includes numerical examples and analyses that illustrate how the proposed algorithms perform under various large-size real-world conditions. Section 5.4 conducts the statistical test to evaluate the performance of the proposed method in more detail—finally, section 5.5 details parameter sensitivity analyses.

5.1 Analysing the performance of the model and algorithms in small-size problems

There are ten problems of varied dimensions to test the performance of the algorithms and the model proposed. The outputs of meta-heuristics are compared to the GAMS results achieved using AUGMECON. As presented in Table 4, the proposed meta-heuristics' objective function values (OFV) and errors are reported for each problem compared to the AUGMECON. The maximum run time for meta-heuristic algorithms has been set to 3600 s. In this paper, the error rate of each algorithm in comparison to the AUGMECON is determined using the following

Table 4: Results obtained by AUGMECON, NSGA-II, and MOEA/D.

(Problem no., depots, affected areas, time period, product no.)	AUGMECON		NSGA-II		Gap (%)	MOEA/D		Gap (%)
	Best OF (1,2,3)	CPU time	Best OF (1,2,3)	CPU time	OF (1,2,3)	Best OF (1,2,3)	CPU time	OF (1,2,3)
(1,2,5,3,2)	(74.7,8.4,43)	284	(74.7, 8.4,43)	426	(0.000,0.000,0.000)	(74.7,8.4,43)	472	(0.000,0.000,0.000)
(2,3,10,3,2)	(82.3,13.2,37)	573	(83,11.3,39)	661	(0.009,0.144,0.054)	(82.5,12.6,38)	682	(0.002,0.045,0.027)
(3,4,9,3,2)	(80.9,14,58)	825	(84.1,12.6,63)	837	(0.040,0.100,0.086)	(84.1,13.1,62)	819	(0.040,0.064,0.069)
(4,3,12,4,3)	(101.4,18.8,79)	1135	(107.9,18.1,82)	1023	(0.064,0.037,0.038)	(107.9,17.6,82)	963	(0.064,0.064,0.038)
(5,5,14,4,3)	(107.3,10.3,86)	1637	(110.4,10.1,87)	1251	(0.029,0.019,0.012)	(110.4,9,89)	1104	(0.029,0.126,0.035)
(6,6,15,5,3)	(128.1,17.4,123)	2563	(135.6,15.7,127)	1386	(0.059,0.098,0.033)	(135.6,16.3,129)	1284	(0.059,0.063,0.049)
(7,7,17,5,4)	(136.8,14.4,109)	3048	(141.9,13.2,124)	1503	(0.037,0.083,0.138)	(141.9,13.9,114)	1403	(0.037,0.035,0.046)
(8,8,18,6,4)	(-,-,-)	-	(174.3,18.3,149)	1783	(-,-,-)	(174.3,17.9,151)	1583	(-,-,-)
(9,9,19,6,5)	(-,-,-)	-	(186.3,16,156)	1980	(-,-,-)	(186.3,18.3,149)	1792	(-,-,-)
(10,10,21,8,5)	(-,-,-)	-	(219.6,14.9,173)	2194	(-,-,-)	(219.6,14.8,172)	1941	(-,-,-)
Average	**(203.3,27.57,76.43)**	**284**	**(131.78,13.86,104.3)**		**(3.38,6.88,5.14)%**	**(131.73,14.19,102.9)**		**(3.30,5.68,3.76)%**

Algorithm 2: *NSGA-II Algorithm*

Generate the initial population A_ξ ;
Set the iteration $\xi = 1$;
while $\xi \leq \xi_{max}$ *Do*
  Apply the crossover and mutation to A_ξ *to generate new solutions* B_ξ ;
  Merge A_ξ *and* B_ξ *as total population* T_ξ ;
  Rank solutions in T_ξ *in Pareto front;*
  Choose best N_p *population from* T_ξ *as* $A_{\xi+1}$ *with crowding distance function;*
  $\xi = \xi + 1$
end

Algorithm 3: *MOEA/D Algorithm*

Initialization of generation A_ξ ;
for $i \in \{1 \ldots, \mu\}$
  Set the neighbourhood index list $B^i = \{i_1, \ldots, i_T\}$
end
Initialization of iteration $\xi = 1$;
while generation $\xi \leq \xi_{max}$
  for $i \in \{1 \ldots, \mu\}$
    Randomly select two indices k and l from B^i;
    Generate a child u^i *by crossing* x^k *and* x^l;
    Apply a mutation operator to u^i;
    for $j \in B^i$
      If $g(u^i|w^j, z^*) \leq g(x^j|w^j, z^*)$
        $x^j \leftarrow u^i$
      end
    end
  end
  $\xi = \xi + 1$
end

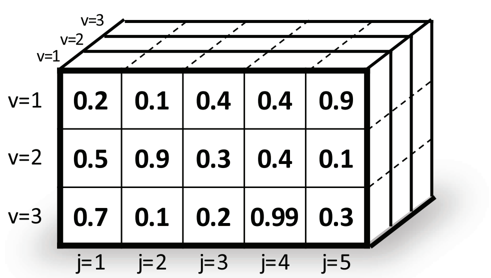

Figure 5: A schematic sample of the solution representation.

equations for each objective function of the mathematical model (Yazdani *et al.*, 2017):

$$\mathrm{Gap}_{OF_i} = \frac{OF_{i\,Metahurestic} - OF_{i\,AUGMECON}}{OF_{i\,AUGMECON}} \times 100, \qquad i = 1, 2, 3 \quad (26)$$

where $OF_{i\,Metahurestic}$ is the best results obtained by the meta-heuristic for objective i, while $OF_{i\,AUGMECON}$ is the obtained result for objective i using the AUGMECON.

The NSGA-II and AUGMECON values differ by 3.38, 6.88, and 5.14% for the first to the third objective functions, respectively. The MOEA/D and AUGMECON have average differences of 3.30, 5.68, and 3.76%, respectively, for the first, second, and third objective functions. The fact that the average gaps of three objective functions are slight leads us to conclude that the meta-heuristic approaches proposed are effective. Figure 7 shows the CPU time needed to solve each meta-heuristic algorithm compared to the AUGMECON. The AUGMECON's solving time grows exponentially in proportion to the problem's size, and for problems 9 and 10, the method was not able to solve the problem. In contrast, meta-heuristic algorithms work much faster.

5.2 Metrics used for evaluation

In this work, multiple criteria were utilised to assess the performance of various algorithms in multi-objective optimisa-

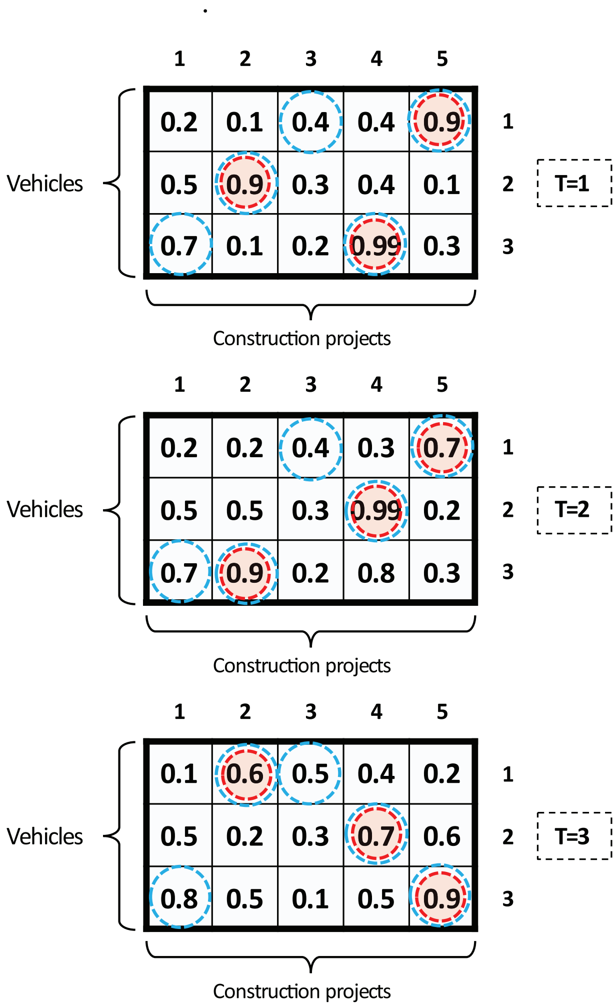

Figure 6: Decoding the solution representation.

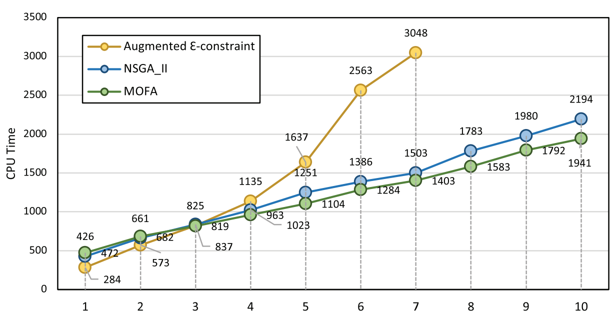

Figure 7: CPU time different approaches.

tion problems where problem solutions incorporate the optimal Pareto front. An algorithm's performance may be evaluated quantitatively by counting the number of Pareto solutions it generates. The larger this number, the better the algorithm. The distance index may also be used to figure out how far apart two solutions are. The better it is if this index has a lower value. The index of distance is determined as follows (Schott, 1995):

$$SM = \frac{\sum_{i=1}^{\mathcal{N}-1} \left|\bar{\mathfrak{d}} - \mathfrak{d}_i\right|}{(\mathcal{N}-1)\,\bar{\mathfrak{d}}}, \tag{27}$$

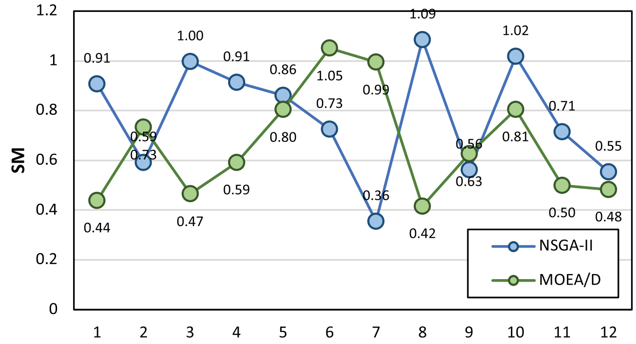

Figure 8: Comparison between NSGA-II and MOEA/D according to the spacing metric.

where d is the average of dis, N is the total number of Pareto solutions, and d_i is the distance between two successive solutions in the optimum front obtained by each method. The variety index is another way to measure the diversity of possible solutions, and its larger values are more suitable. Calculating this index is as follows (Zitzler & Thiele, 1999):

$$DM = \sqrt{\left(\frac{\max f_{1i} - \min f_{1i}}{f_{1,total}^{max} - f_{1,total}^{min}}\right)^2 + \left(\frac{\max f_{2i} - \min f_{2i}}{f_{2,total}^{max} - f_{2,total}^{min}}\right)^2}. \tag{28}$$

In total, 12 problems of varied sizes were created, the performance of two meta-heuristic methods was compared, and Pareto-optimal solutions were generated for each. Tables 5 and 6 list the created sample problems, failure times, fuzzy demands, and the values of evaluation metrics for methods.

The number of ground vehicles ranges between three and ten, while the number of air vehicles ranges between two and five. There is a single warehouse for air vehicles in all situations. The capacity and transportation time parameters are produced using the uniform distributions between 50–60 and 8–20, respectively. The demand is represented by a triangle fuzzy number with the structure $\mathcal{Q} = (\mathcal{Q}_1, \mathcal{Q}_2, \mathcal{Q}_3)$, which generates using uniform distributions: $\mathcal{Q}_1$ from [20, 45], $\mathcal{Q}_2$ from [46, 70], and $\mathcal{Q}_3$ from [71, 140]. Additionally, the travel time of vehicles used to distribute goods is considered to be generated using a uniform distribution. We have a scenario matrix for each problem, in which the rows represent scenarios, the columns represent vehicles, and the numbers in the table represent the failure time of vehicles. That is highlighted in the table as $\delta_{24}^{3} = 16$, indicating that vehicle 2, in period 4, in scenario three, breaks down after 16 h, resulting in undelivered materials to projects.

The parameters of the algorithms presented in Table 7 are given after tuning the parameters in the proposed algorithms using the response surface methodology (RSM) method.

5.3 Analysing the performance of the model and algorithms in small-size problems

In Table 8, all the problems generated in Table 5 are solved separately by the algorithm, and the values of the standard indicators used are reported. To better evaluate the algorithms' performances, each indicator is shown schematically in Figs. 8 to 10.

In order to gain a better understanding of how well the meta-heuristic algorithms perform, the following computations are shown to illustrate the results of comparison metrics. With the spacing metric, we can see that the MOEA/D outperforms the NSGA-II when compared to the other meta-heuristic algorithms in Fig. 8.

Table 5: Values for generating sample problems.

Problem no.	Projects with accessible roads	Projects with damaged roads	Vehicle depot	Truck	Helicopter	Types of materials	Periods
1	7	5	6	3	2	2	2
2	10	7	6	3	2	3	2
3	15	9	7	4	2	4	2
4	16	7	7	4	2	3	3
5	18	8	7	5	3	4	3
6	20	8	8	6	3	5	3
7	24	10	8	6	3	4	4
8	25	11	9	5	4	5	4
9	30	15	9	7	4	6	4
10	33	16	9	7	5	4	5
11	35	20	10	9	5	5	5
12	40	25	10	10	5	6	5

Table 6: The failure rates of vehicles and the fuzzy demand in various scenarios.

$\tilde{\mathcal{Q}} = (\mathcal{Q}_1, \mathcal{Q}_2, \mathcal{Q}_3)$	Vehicle 5	Vehicle 4	Vehicle 3	Vehicle 2	Vehicle 1	Scenario
(20,46,75)	10	16	13	7	10	1
(25,50,80)	10	9	14	4	20	2
(30,53,95)	16	8	11	16	10	3
(35,60,100)	10	20	7	10	10	4
(45,70,120)	8	10	9	10	15	5

Table 7: Tunned parameters.

Algorithms	Parameters	Small-size problems	Large-size problems
NSGA-II	Maximum number of iterations	73	205
	Population size	51	192
	Crossover rate	0/39	0/34
	Mutation rate	0/16	0/19
	Mu	0/07	0/8
MOEA/D	Maximum number of iterations	97	186
	Population size	38	149
	nArchive	29	101
	Size of neighbourhood	13	20
	Lambda	0/21	0/18

Table 8: Obtained values for different instances by NSGA-II and MOEA/D.

Problem no.	MOEA/D				NSGA-II			
	SM	DM	NOPS	CPU time	SM	DM	NOPS	CPU time
1	7.939933	7.939933	6	615	0.4396193	7.479914	7	652
2	3.18014	3.18014	5	763	0.7331419	7.15122	5	782
3	5.655873	5.655873	6	1043	0.4650282	7.922465	9	1023
4	4.878148	4.878148	9	1245	0.5922232	6.916572	7	1202
5	3.805205	3.805205	6	1684	0.8037516	7.637064	7	1502
6	7.288054	7.288054	7	1943	1.0505771	4.179673	5	1732
7	7.508725	7.508725	8	2692	0.9946069	5.532396	11	2319
8	3.031869	3.031869	9	3042	0.416409	5.124544	6	2548
9	6.712907	6.712907	6	4174	0.6263944	3.038738	7	3657
10	6.978169	6.978169	8	6031	0.8053852	3.411685	9	5662
11	4.955259	4.955259	8	7453	0.4990383	8.496907	7	6650
12	7.859942	7.859942	5	10554	0.4833295	5.1066	8	8636
Average	5.816185	5.816185	6.916667	3436.583	0.6591254	5.999815	7.333333	3030.4167

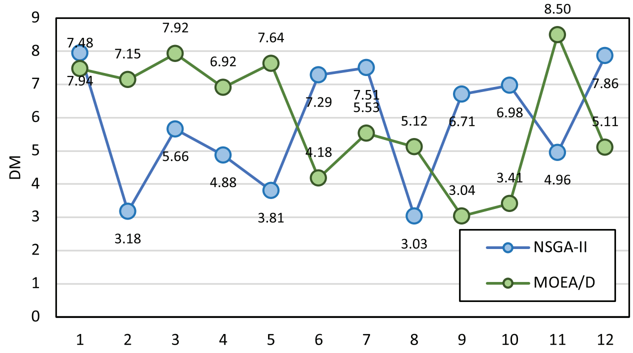

Figure 9: Comparison between NSGA-II and MOEA/D according to the diversity metric.

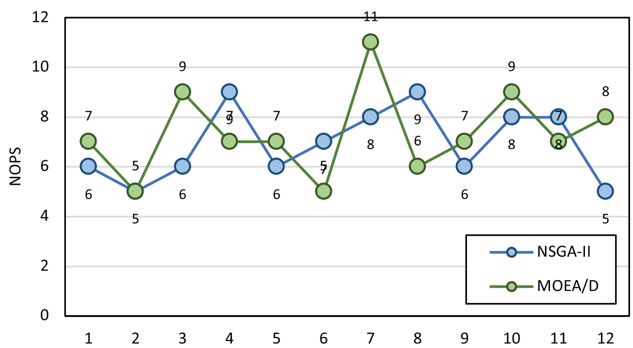

Figure 10: Comparison between NSGA-II and MOEA/D according to the number of Pareto solutions.

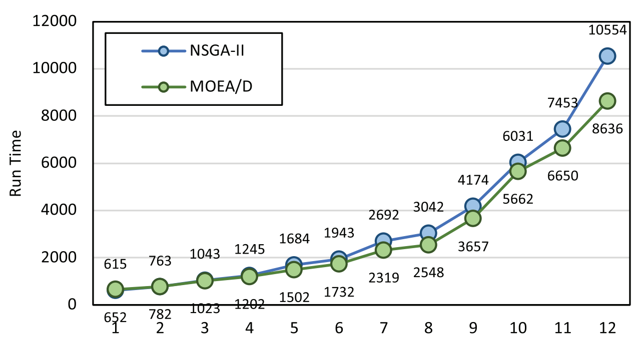

Figure 11: Comparison between NSGA-II and MOEA/D according to CPU time.

Comparing solution times shows that the MOEA/D finds better solutions faster, resulting in better overall performance. (Fig. 11).

The results of the diversity metric shown in Fig. 9 demonstrate that there is no particular trend for the algorithms.

The number of Pareto solutions determined by the MOEA/D is depicted in Fig. 10, demonstrating its superior performance.

5.4 Statistical test

For each comparison metric, a number of statistical tests were conducted to see if there was any statistically significant difference between the two methods. The results of the independent *t*-test to compare the proposed algorithms are provided in Tables 9 and 10.

According to the results reported in Table 9, it can be seen that the significant level of Levene's test for equality of variances for SM, DM, NOPS, and Run indices are 0.795, 0.770, 0, and 0. The resulting p-values of Levene's test for SM and DM are greater than significance level 0.05, indicating that the null hypothesis of equal variances is not rejected, and no difference between the variances is concluded. While the P-values obtained from Levene's test for NOPS and Run are less than the significance level of 0.05. As a result, the null hypothesis of equal variances is rejected, and it is concluded that the variances differ.

Based on the significant level of the independent *t*-test, the obtained values for DM and SM are 0.623 and 0.286, which are both greater than 5%. As a result, the mean of the two samples is not significantly different, and the ability of both algorithms in the SM, DM criteria is not significantly different. In contrast, the obtained values for NOPS and Run are 0.002 and 0.003, respectively, which are less than 5%, so the assumption of the equal mean of the two samples is rejected. In NOPS criteria, the algorithm with the highest value is preferred. As a result, the MOEA/D algorithm outperforms the NSGA-II algorithm. In the Run criteria, however, the algorithm with the shortest run time is preferred. The NSGA-II method's average value (3693.0909) is lower than the MOEA/D method's (7.3333). As a result, the NSGA-II algorithm outperforms the MOEA/D algorithm.

5.5 Sensitivity analysis

The sensitivity analysis is taken into account in solving problem 6. Tables 8 and 9 show the results of changing demand and vehicle capacity at the same time, as well as the mean failure time of the vehicles.

As shown in Table 11, there will be no change in OFV or route selection if we simultaneously reduce demand and increase vehicle capacity. When we simultaneously increase material demand while decreasing vehicle capacity, we will see that transportation times and undelivered materials to projects (shortage due to delays and failures) will increase, as will the objective function, with the exception of one case that will remain constant. Obviously, with increasing demand and decreasing vehicle capacity, more vehicles will be required to service, increasing transportation time (objective function 1) and the likelihood of vehicle failure. As a result, the level of shortage (objective function 3) will rise. On the other hand, the likelihood of taking less reliable routes will rise. If demand remains constant while reducing vehicle capacity, we effectively reduce overcapacity, and the routeing will not change again. However, all three objective functions will be altered if demand remains constant and vehicle capacity is reduced from 0.9 to 0.8. For instance, vehicle one previously had to serve three projects due to its reduced capacity (0.8), but it will no longer be able to do so due to its reduced capacity (0.8), so this task will be assigned to vehicle 2. When machine 2 wishes to travel through the arc, the transport time (objective function 1) increases and becomes non-optimal. Second, in various scenarios, the delays in meeting demand (objective function 3) increase. Third, the previously chosen arc had higher reliability, which was reduced from 10.3 to 10.1 by making this change and by lowering the capacity to 0.7. Now, if we assume the vehicle's capacity is fixed and reduce the demand, the route will not change, nor will the objective functions 1 (transport time) and 2 (reliability), but objective function 3 (undelivered materials to projects) will decrease because we reduced the demand. As a result, all of the demands will be met. However, if we increase the demand, the vehicle will be unable to meet this level of demand due to constant capacity and increasing demand. As a result, transportation time (objective 1) will increase while reliability (objective 2) will decrease. As a result, the

Table 9: Results of statistical hypothesis test to compare the performance of algorithms (independent *t*-test).

		Levene's test for equality of variances		t-Test for equality of means						
		F	Sig.	t	df	Sig. (2-tailed)	Mean difference	Std. error difference	95% Confidence interval of the difference	
									Lower	Upper
SM	Equal variances assumed	0.069	0.795	1.094	21	0.286	0.10257	0.09375	−0.09239	0.29753
	Equal variances not assumed			1.091	20.502	0.288	0.10257	0.09403	−0.09325	0.29840
DM	Equal variances assumed	0.087	0.770	−0.498	21	0.623	−0.37670	0.75596	−1.94881	1.19541
	Equal variances not assumed			−0.499	20.950	0.623	−0.37670	0.75450	−1.94600	1.19261
NOPS	Equal variances assumed	22.911	0.000	−3.841	21	0.001	−3023.41667	787.21206	−4660.51377	−1386.31956
	Equal variances not assumed			−4.019	11.000	0.002	−3023.41667	752.20719	−4679.01339	−1367.81994
RUN	Equal variances assumed	22.930	0.000	4.108	21	0.001	3685.75758	897.27824	1819.76532	5551.74983
	Equal variances not assumed			3.924	10.000	0.003	3685.75758	939.21166	1593.06374	5778.45141

Table 10: Statistical characteristics of the three criteria for both algorithms (independent *t*-test).

	Method	N	Mean	Std. deviation	Std. error mean
SM	NSGA-II	11	0.7617	0.23212	0.06999
	MOEA/D	12	0.6591	0.21751	0.06279
DM	NSGA-II	11	5.6231	1.77043	0.53381
	MOEA/D	12	5.9998	1.84714	0.53322
NOPS	NSGA-II	11	7.0000	1.48324	0.44721
	MOEA/D	12	3030.4167	2605.72169	752.20706
RUN	NSGA-II	11	3693.0909	3115.01225	939.21153
	MOEA/D	12	7.3333	1.72328	0.49747

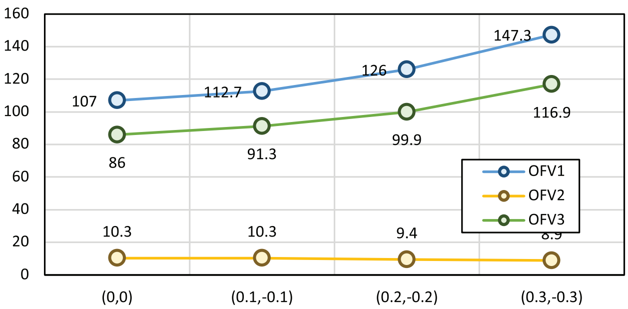

Figure 18. Sensitive analysis when the capacity decreases and demand increases.

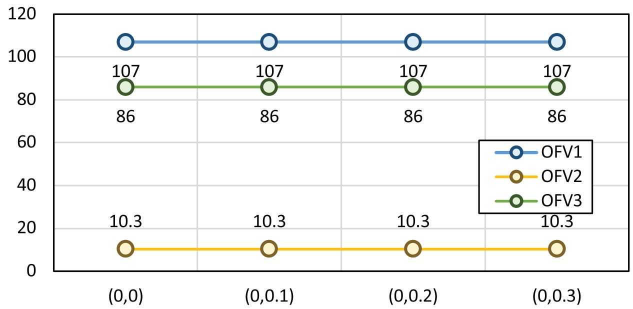

Figure 13. Sensitive analysis when the demand is constant and capacity increases.

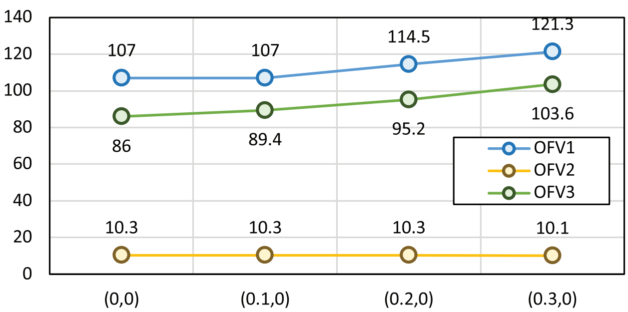

Figure 12. Sensitive analysis when the capacity is constant and demand increases.

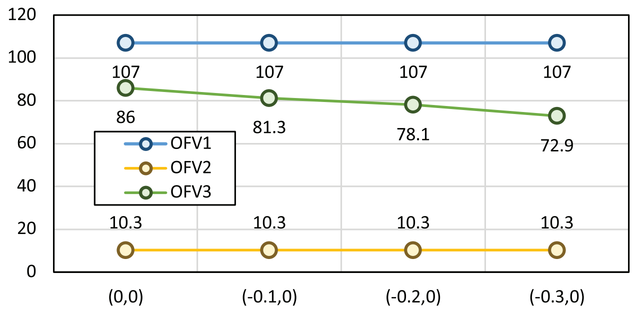

Figure 14. Sensitive analysis when the capacity is constant and demand decreases.

duration of the delay (undelivered materials to projects) (objective 3 function) will increase.

Table 12 shows the sensitivity analysis results based on changes in the average vehicle failure time. Figures 11–19 show the results of a sensitivity analysis of simultaneous changes in demand and vehicle capacity. [Note: The amount of change in demand and capacity is shown as ($\Delta Dem,\ \Delta Cap$).]

According to Table 12, we can expect the parameters related to vehicle breakdown times to decrease as the average vehicle breakdown time increases. They perform better by increasing the breakdown time from 1 to 1.1 and because the vehicle has a longer breakdown time. It attempts to select routes that were previously damaged in those vehicles and had an unmet demand that it did not select. When we reduce the average vehicle breakdown time, the model tries to increase the vehicle breakdown time, but the vehicle breakdown rate is very high. Figures 20 and 21 depict the sensitivity analysis as a result of changes in average vehicle breakdown time. [Note: The amount of change in demand and capacity is show as ($\Delta Dem,\ \Delta Cap$).]

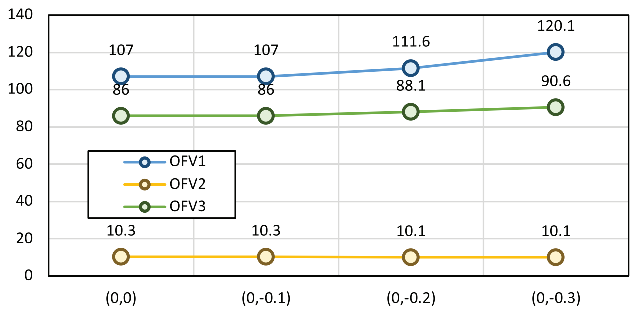

Figure 15. Sensitive analysis when the demand is constant and capacity decreases.

6. Conclusions and Future Works

Reconstruction projects following a destructive disaster can be challenging due to time and resources constraints. A large number of post-disaster reconstruction efforts are compromised by inadequate planning. Consequently, this paper proposed an integrated model for delivering materials to the location of re-

Table 11: Sensitivity analysis of vehicle capacity and demand variations at the same time.

Capacity	Demand																				
	−0.3			−0.2			−0.1			0			0.1			0.2			0.3		
	OF1	OF2	OF3	OF1	OF2	OF3	OF1	OF2	OF3	OF1	OF2	OF3	OF1	OF2	OF3	OF1	OF2	OF3	OF1	OF2	OF3
0.7	107	10.3	72.9	107	10.3	80.5	113.7	10.1	84.9	120.1	10.1	90.6	127.4	9.7	96.1	134.2	9.2	104.2	147.3	8.9	116.9
0.8	107	10.3	72.9	107	10.3	78.1	107	10.3	83.6	111.6	10.1	88.1	119.4	9.9	93.9	126	9.4	99.9	134.8	9.1	110.8
0.9	107	10.3	72.9	107	10.3	78.1	107	10.3	81.3	107	10.3	86	112.7	10.1	91.3	119.8	10.1	97.2	128.9	9.9	106.5
1	107	10.3	72.9	107	10.3	78.1	107	10.3	81.3	107	10.3	86	107	10.3	89.4	114.5	10.3	95.2	121.3	10.1	103.5
1.1	107	10.3	72.9	107	10.3	78.1	107	10.3	81.3	107	10.3	86	107	10.3	89.4	107	10.3	93.8	115.1	10.1	98.1
1.2	107	10.3	72.9	107	10.3	78.1	107	10.3	81.3	107	10.3	86	107	10.3	89.4	107	10.3	93.1	107	10.3	96.4
1.3	107	10.3	72.9	107	10.3	78.1	107	10.3	81.3	107	10.3	86	107	10.3	89.4	107	10.3	93.1	107	10.3	96.4

Table 12: Sensitivity analysis of vehicle failure time variations.

Mean of vehicle's failure time	−0.7	−0.6	−0.5	−0.4	−0.3	−0.2	−0.1	0	0.1	0.2	0.3	0.4	0.5	0.6	0.7
OFV1	126.8	126.6	125.1	121.0	120.2	109.5	107.5	107.0	104.3	98.7	96.3	94.2	91.2	91.2	91.2
OFV2	9.4	9.4	9.4	9.8	10.1	10.1	10.3	10.3	10.3	10.5	10.5	10.7	10.7	10.7	10.7
OFV3	103.4	103.4	103.3	101.8	99.1	95.1	91.2	86.0	81.7	78.7	75.1	73.9	73.9	73.8	73.8

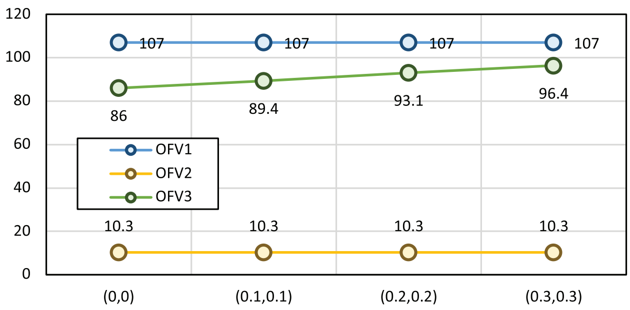

Figure 16. Sensitive analysis when the capacity increases and demand increases.

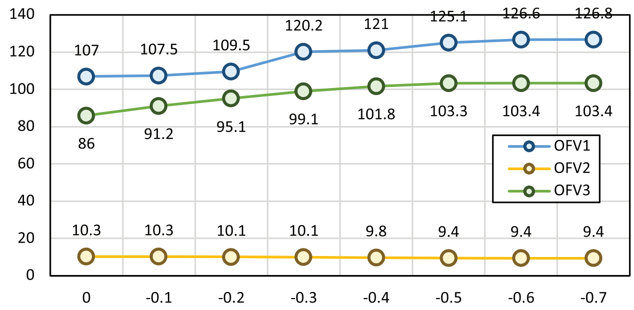

Figure 21. Sensitive analysis when the average failure time of vehicle increases.

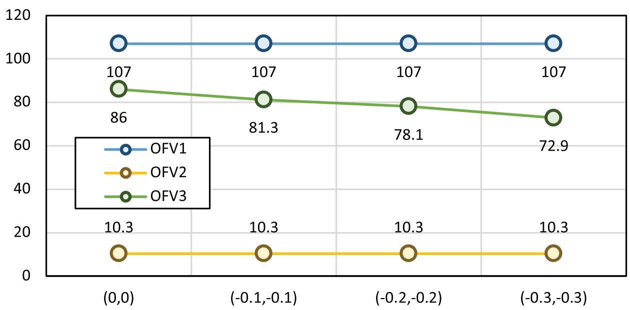

Figure 17. Sensitive analysis when the capacity decreases and demand decrease.

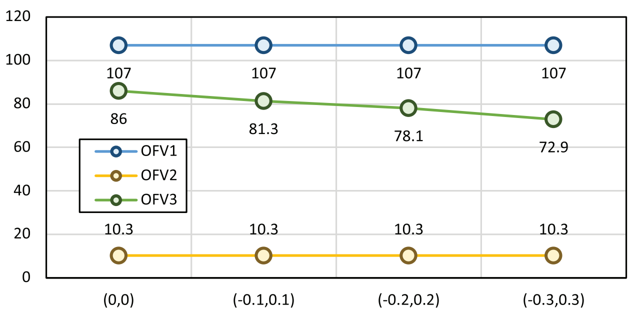

Figure 19. Sensitive analysis when the capacity increase and demand decreases.

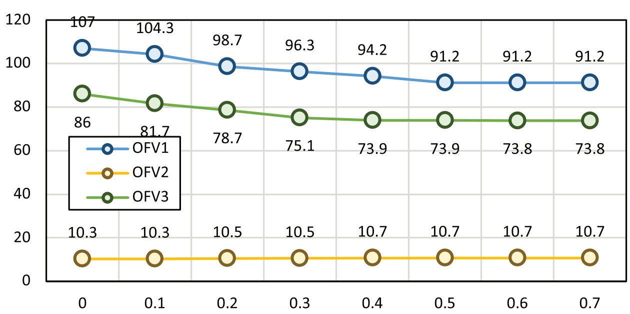

Figure 20. Sensitive analysis when the average failure time of vehicle decrease.

construction projects following a large-scale disaster. Clustering the location of construction projects through the use of the proposed DE-K-prototypes method and designing the most reliable route for trucks through the use of a decision-making approach and graph theory (Permanent matrix) were two suggested approaches for designing a reliable system for delivering construction materials to the reconstruction projects. Consideration of concurrent disruptions in distribution operations is a necessity that is frequently overlooked, resulting in deficiency and delay in the process of distributing construction materials. Thus, in order to avoid disruptions in the route of trucks, serving and distribution to the construction projects were prioritised (in terms of the factors affecting route reliability), and, on the other hand, a strategy was adopted in which, in order to minimise the total weighted undelivered materials to projects, trucks were scheduled under various scenarios so that, in the event of a disruption, the distribution system and also the serenity are not damaged.

We attempted to minimise both total travel time and shortage in this research by proposing a clustered and disrupted vehicle routeing model. As a result, a model was developed in which disparate vehicles from multiple depots initiated relief operations on the ground and in the air and delivered construction material to the projects. The optimal solution was found using the AUGMECON in a small size. Considering the complexity of the problem, two algorithms were proposed, including an NSGA-II and a MOEA/D, to solve the problems in large-size instances.

The mean difference between the objective values of the NSGA-II and the epsilon-constraint method was 3.38 for the first objective function (transport time), 6.88 for the second objective function (reliability), and the same difference for the third objective function (the total weighted undelivered materials to projects) is 5.14%. We found that the average gaps of the three objective functions with meta-heuristic algorithms are very small. As the size of the problem increases, the time to solve the epsilon-constraint method increases exponentially to the extent that it is unable to respond from problem 8 onwards, while the execution time of meta-heuristic algorithms increases with a slight incline and is capable even with relatively slight slopes. NSGA-II and MOEA/D have the same capability in terms of SM and DM, but MOEA/D has a better performance in terms of NOPS than NSGA-II. And NSGA-II has better performance in terms of CPU time than MOEA/D.

Providing decision makers with a set of reliable solutions to help them make decisions about the delivery of construction materials to post-disaster reconstruction projects is one of the most important management insights that can be considered in this research. With the help of this study's advanced approach, planners will be able to find the best solution to the problem. The results of the sensitivity analysis of the model show that if the demand of the projects decreases and at the same time the capacity of the vehicles increases or remains constant, almost no change will occur in all three objective functions and the optimal routes will remain unchanged. The capacity of the vehicle will remain constant (decrease). In most of the time, vehicles distribute several types of materials in a few periods, in which the probability of using less reliable routes will increase, and as a result, due to the slow process and the possibility of equipment failure, the undelivered materials to projects will increase. If we increase the demand for construction projects and at the same time reduce the capacity of vehicles, the duration of operation will be longer and vehicles will provide assistance on less reliable routes, and as a result, the undelivered materials to projects will increase. Managers and decision makers should specify potential warehouse locations in more secure areas to avoid the use of expensive transportation modes or less reliable access roads, in light of the project's sensitivity to construction material. Additionally, managers and decision makers are encouraged to outsource certain tasks to reputable contractors.

Many studies in disaster risk management have their own set of limitations. This study is no exception. Generally, there is no reliable database to define the values of the model's parameters; thus, in this study, some parameters were obtained after consulting with experts and others were generated randomly. Furthermore, uncertainty was addressed in the problem only for a subset of parameters, whereas in the real world, other parameters are associated with uncertainty. Additionally, while many multi-objective meta-heuristic algorithms exist in the literature that may perform better, only NSGA-II and MOEA/D were used.

Finally, some future research directions are possible. To begin, nondeterministic values can be investigated for other model parameters. Additionally, employing other multi-objective metahurestic algorithms or even developing some exact or semi-exact methods such as benders decomposition algorithm can be investigated in the future. Developing various variants of uncertainty approaches such as fuzzy programming and robust optimisation, grey systems, and stochastic optimal control to address the problem's uncertain nature can be an interesting research area. Another suggestion for future research is to incorporate inventory decisions into the proposed model in order to optimise the problem more practically.

Conflict of Interest Statement

None declared.

References

Abioye, O. F., Dulebenets, M. A., Ozguven, E. E., Moses, R., Boot, W. R., & Sando, T. (2020). Assessing perceived driving difficulties under emergency evacuation for vulnerable population groups. *Socio-Economic Planning Sciences*, *72*, 100878.

Alisjahbana, I., Graur, A., Lo, I., & Kiremidjian, A. (2022). Optimizing strategies for post-disaster reconstruction of school systems. *Reliability Engineering & System Safety*, *219*, 108253. https://doi.org/10.1016/j.ress.2021.108253.

Babaeinesami, A., Tohidi, H., Ghasemi, P., Goodarzian, F., & Tirkolaee, E. B. (2022). A closed-loop supply chain configuration considering environmental impacts: A self-adaptive NSGA-II algorithm. *Applied Intelligence*. https://doi.org/10.1007/s10489-021-02944-9.

Bahmani, H., & Zhang, W. (2021a). Application of system thinking and factors interrelationship analysis to identify primary success factors of post-natural disaster recovery projects. *Sustainability*, *13*, 3392.

Bahmani, H., & Zhang, W. (2021b). Comprehensive success evaluation framework for socio-natural disaster recovery projects. *Buildings*, *11*, 647. https://www.mdpi.com/2075-5309/11/12/647.

Bahmani, H., & Zhang, W. (2022a). A conceptual framework for integrated management of disasters recovery projects. *Natural Hazards*. https://doi.org/10.1007/s11069-022-05328-5.

Bahmani, H., & Zhang, W. (2022b). Why do communities recover differently after socio-natural disasters? Pathways to comprehensive success of recovery projects based on bam's (Iran) neighborhoods' perspective. *International Journal of Environmental Research and Public Health*, *19*, 678.

Barakat, S. (2003). Housing reconstruction after conflict and disaster. *Humanitarian Policy Group, Network Papers*, *43*, 1–40.

Baykasoglu, A. (2014). A review and analysis of "graph theoretical-matrix permanent" approach to decision making with example applications. *Artificial Intelligence Review*, *42*, 573–605.

Bilau, A. A., Witt, E., & Lill, I. (2017). Analysis of measures for managing issues in post-disaster housing reconstruction. *Buildings*, *7*, 29.

Celentano, G., Escamilla, E. Z., Göswein, V., & Habert, G. (2019). A matter of speed: The impact of material choice in post-disaster reconstruction. *International Journal of Disaster Risk Reduction*, *34*, 34–44. https://doi.org/10.1016/j.ijdrr.2018.10.026.

Chang, Y., Wilkinson, S., Potangaroa, R., & Seville, E. (2010). Resourcing challenges for post-disaster housing reconstruction: A comparative analysis. *Building Research & Information*, *38*, 247–264.

Charles, S. H., Chang-Richards, A. Y., & Yiu, T. W. (2022). A systematic review of factors affecting post-disaster reconstruction projects resilience. *International Journal of Disaster Resilience in the Built Environment*, *13*, 113–132. https://doi.org/10.1108/IJDRBE-10-2020-0109.

Chen, Q., Ge, Y.-E., Lau, Y.-y., Dulebenets, M. A., Sun, X., Kawasaki, T., Abderrahman, A., & Tao, X. (2022). Effects of COVID-19 on passenger shipping activities and emissions: Empirical analysis of passenger ships in Danish waters. *Maritime Policy & Management*, 1–21. https://doi.org/10.1080/03088839.2021.2021595.

Copping, A., Kuchai, N., Hattam, L., Paszkiewicz, N., Albadra, D., Shepherd, P., Burat, E.S., & Coley, D. (2022). Understanding material and supplier networks in the construction of disaster-relief shelters: The feasibility of using social network analysis as a decision-making tool. *Journal of Humanitarian Logistics and Supply Chain Management*, 12, 78–105. https://doi.org/10.1108/JHLSCM-01-2020-0007.

Deb, K., Pratap, A., Agarwal, S., & Meyarivan, T. (2002). A fast and elitist multiobjective genetic algorithm: NSGA-II. *IEEE Transactions on Evolutionary Computation*, *6*, 182–197.

Diaz, R., Behr, J. G., & Acero, B. (2022). Coastal housing recovery in a postdisaster environment: A supply chain perspective.

International Journal of Production Economics, *247*, 108463. https://doi.org/10.1016/j.ijpe.2022.108463.

Dulebenets, M. A. (2021). An adaptive polyploid memetic algorithm for scheduling trucks at a cross-docking terminal. *Information Sciences*, *565*, 390–421.

Dulebenets, M. A., Abioye, O. F., Ozguven, E. E., Moses, R., Boot, W. R., & Sando, T. (2019). Development of statistical models for improving efficiency of emergency evacuation in areas with vulnerable population. *Reliability Engineering & System Safety*, *182*, 233–249.

Dulebenets, M. A., Pasha, J., Abioye, O. F., Kavoosi, M., Ozguven, E. E., Moses, R., Boot, W.R., & Sando, T. (2019). Exact and heuristic solution algorithms for efficient emergency evacuation in areas with vulnerable populations. *International Journal of Disaster Risk Reduction*, *39*, 101114. https://doi.org/10.1016/j.ijdrr.2019.101114.

Enshassi, A., Chatat, T., von Meding, J., & Forino, G. (2017). Factors influencing post-disaster reconstruction project management for housing provision in the Gaza Strip, occupied Palestinian territories. *International Journal of Disaster Risk Science*, *8*, 402–414. https://doi.org/10.1007/s13753-017-0155-4.

Esmaili, M., Amjady, N., & Shayanfar, H. A. (2011). Multi-objective congestion management by modified augmented ε-constraint method. *Applied Energy*, *88*, 755–766.

Fathollahi-Fard, A. M., Woodward, L., & Akhrif, O. (2021a). Sustainable distributed permutation flow-shop scheduling model based on a triple bottom line concept. *Journal of Industrial Information Integration*, *24*, 100233. https://doi.org/10.1016/j.jii.2021.100233.

Fathollahi-Fard, A. M., Dulebenets, M. A., Hajiaghaei–Keshteli, M., Tavakkoli-Moghaddam, R., Safaeian, M., & Mirzahosseinian, H. (2021b). Two hybrid meta-heuristic algorithms for a dual-channel closed-loop supply chain network design problem in the tire industry under uncertainty. *Advanced Engineering Informatics*, *50*, 101418. https://doi.org/10.1016/j.aei.2021.101418.

Geetha, N., & Sekar, P. (2016). Graph theory matrix approach a review. *Indian Journal of Science and Technology*, *9*, 1–4.

Ghannad, P., Lee, Y.-C., Friedland, C. J., Choi, J. O., & Yang, E. (2020). Multiobjective optimization of postdisaster reconstruction processes for ensuring long-term socioeconomic benefits. *Journal of Management in Engineering*, *36*, 04020038.

Ghannad, P., Lee, Y.-C., & Choi, J. O. (2021). Prioritizing postdisaster recovery of transportation infrastructure systems using multiagent reinforcement learning. *Journal of Management in Engineering*, *37*, 04020100. https://doi.org/10.1061/(ASCE)ME.1943-5479.0000868.

Gharib, Z., Tavakkoli-Moghaddam, R., Bozorgi-Amiri, A., & Yazdani, M. (2022). Post-disaster temporary shelters distribution after a large-scale disaster: An integrated model. *Buildings*, *12*, 414. https://doi.org/10.3390/buildings12040414.

Habibi Rad, M., Mojtahedi, M., & Ostwald, M. J. (2021a). Industry 4.0, disaster risk management and infrastructure resilience: A systematic review and bibliometric analysis. *Buildings*, *11*, 411.

Habibi Rad, M., Mojtahedi, M., & Ostwald, M. J. (2021b). The integration of lean and resilience paradigms: A systematic review identifying current and future research directions. *Sustainability*, *13*, 8893.

Habibi Rad, M., Mojtahedi, M., Ostwald, M. J., & Wilkinson, S. (2022). A conceptual framework for implementing lean construction in infrastructure recovery projects. *Buildings*, *12*, 272. https://doi.org/10.3390/buildings12030272

Huang, R., Malik, A., Lenzen, M., Jin, Y., Wang, Y., Faturay, F., & Zhu, Z. (2021). Supply-chain impacts of Sichuan earthquake: A case study using disaster input–output analysis. *Natural Hazards*, 1–22.

Huang, R., Malik, A., Lenzen, M., Jin, Y., Wang, Y., Faturay, F., & Zhu, Z. (2022). Supply-chain impacts of Sichuan earthquake: A case study using disaster input–output analysis. *Natural Hazards*, *110*, 2227–2248. https://doi.org/10.1007/s11069-021-05034-8.

Huang, Z. (1997). Clustering large data sets with mixed numeric and categorical values. In *Proceedings of the 1st Pacific-Asia Conference on Knowledge Discovery and Data Mining, (PAKDD)* (pp. 21–34). World Scientific Press.

Ji, J., Pang, W., Li, Z., He, F., Feng, G., & Zhao, X. (2020). Clustering mixed numeric and categorical data with cuckoo search. *IEEE Access*, *8*, 30988–31003.

Jiménez, M., Arenas, M., Bilbao, A., & Rodrı, M. V. (2007). Linear programming with fuzzy parameters: An interactive method resolution. *European Journal of Operational Research*, *177*, 1599–1609.

Khodahemmati, N., & Shahandashti, M. (2020). Diagnosis and quantification of postdisaster construction material cost fluctuations. *Natural Hazards Review*, *21*, 04020019.

Mahtab, Z., Azeem, A., Ali, S. M., Paul, S. K., & Fathollahi-Fard, A. M. (2021). Multi-objective robust-stochastic optimisation of relief goods distribution under uncertainty: A real-life case study. *International Journal of Systems Science: Operations & Logistics*, 1–22. https://doi.org/10.1080/23302674.2021.1879305.

Mavrotas, G. (2009). Effective implementation of the ε-constraint method in multi-objective mathematical programming problems. *Applied Mathematics and Computation*, *213*, 455–465. https://doi.org/10.1016/j.amc.2009.03.037.

Mohaghar, A., Fagheyi, M. S., Moradi-Moghadam, M., & Ahangari, S. S. (2013). Integration of fuzzy GTMA and logarithmic fuzzy preference programming for supplier selection. *Report and Opinion*, *5*, 9–16.

Mohammadnazari, Z., Mousapour Mamoudan, M., Alipour-Vaezi, M., Aghsami, A., Jolai, F., & Yazdani, M. (2022). Prioritizing post-disaster reconstruction projects using an integrated multi-criteria decision-making approach: A case study. *Buildings*, *12*, 136.

Nasiri, M., & ShisheGar, S. (2014). Disaster relief routing by considering heterogeneous vehicles and reliability of routes using an MADM approach. *Uncertain Supply Chain Management*, *2*, 137–150.

Pasha, J., Dulebenets, M. A., Kavoosi, M., Abioye, O. F., Wang, H., & Guo, W. (2020). An optimization model and solution algorithms for the vehicle routing problem with a "factory-in-a-box". *IEEE Access*, *8*, 134743–134763.

Pasha, J., Elmi, Z., Purkayastha, S., Fathollahi-Fard, A. M., Ge, Y.-E., Lau, Y.-Y., & Dulebenets, M. A. (2022). The drone scheduling problem: A systematic state-of-the-art review. *IEEE Transactions on Intelligent Transportation Systems*, 1–24. https://doi.org/10.1109/TITS.2022.3155072.

Pescador-Rojas, M., Hernández Gómez, R., Montero, E., Rojas-Morales, N., Riff, M.-C., & Coello Coello, C. A. (2017). An overview of weighted and unconstrained scalarizing functions. In *International Conference on Evolutionary Multi-Criterion Optimization* (pp. 499–513). Springer.

Platt, S., & So, E. (2017). Speed or deliberation: A comparison of post-disaster recovery in Japan, Turkey, and Chile. *Disasters*, *41*, 696–727.

Rao, R. V., & Padmanabhan, K. K. (2007). Rapid prototyping process selection using graph theory and matrix approach. *Jour-*

nal of Materials Processing Technology, *194*, 81–88. https://doi.org/10.1016/j.jmatprotec.2007.04.003.
Rouhanizadeh, B., & Kermanshachi, S. (2020). Post-disaster reconstruction of transportation infrastructures: Lessons learned. *Sustainable Cities and Society*, *63*, 102505. https://doi.org/10.1016/j.scs.2020.102505.
Safapour, E., & Kermanshachi, S. (2021). Uncertainty analysis of rework predictors in post-hurricane reconstruction of critical transportation infrastructure. *Progress in Disaster Science*, *11*, 100194. https://doi.org/10.1016/j.pdisas.2021.100194.
Schott, J. R. (1995). *Fault tolerant design using single and multicriteria genetic algorithm optimization*. Massachusetts Institute of Technology.
Siriwardhana, S. D., Kulatunga, U., Samaraweera, A., & Shanika, V. G. (2021). Cultural issues of community resettlement in post-disaster reconstruction projects in Sri Lanka. *International Journal of Disaster Risk Reduction*, *53*, 102017.
Theophilus, O., Dulebenets, M. A., Pasha, J., Lau, Y.-y., Fathollahi-Fard, A. M., & Mazaheri, A. (2021). Truck scheduling optimization at a cold-chain cross-docking terminal with product perishability considerations. *Computers & Industrial Engineering*, *156*, 107240. https://doi.org/10.1016/j.cie.2021.107240.
Tirkolaee, E. B., Goli, A., Hematian, M., Sangaiah, A. K., & Han, T. (2019). Multi-objective multi-mode resource constrained project scheduling problem using Pareto-based algorithms. *Computing*, *101*, 547–570. https://doi.org/10.1007/s00607-018-00693-1.
Tirkolaee, E. B., Aydın, N. S., Ranjbar-Bourani, M., & Weber, G.-W. (2020a). A robust bi-objective mathematical model for disaster rescue units allocation and scheduling with learning effect. *Computers & Industrial Engineering*, *149*, 106790. https://doi.org/10.1016/j.cie.2020.106790.
Tirkolaee, E. B., Goli, A., Faridnia, A., Soltani, M., & Weber, G.-W. (2020b). Multi-objective optimization for the reliable pollution-routing problem with cross-dock selection using Pareto-based algorithms. *Journal of Cleaner Production*, *276*, 122927. https://doi.org/10.1016/j.jclepro.2020.122927.
Tirkolaee, E. B., Goli, A., Gütmen, S., Weber, G.-W., & Szwedzka, K. (2022). A novel model for sustainable waste collection arc routing problem: Pareto-based algorithms. *Annals of Operations Research*. https://doi.org/10.1007/s10479-021-04486-2.
Uddin, K., & Matin, M. A. (2021). Potential flood hazard zonation and flood shelter suitability mapping for disaster risk mitigation in Bangladesh using geospatial technology. *Progress in Disaster Science*, *11*, 100185. https://doi.org/10.1016/j.pdisas.2021.100185.
Wang, Z., Zhang, Q., Zhou, A., Gong, M., & Jiao, L. (2015). Adaptive replacement strategies for MOEA/D. *IEEE Transactions on Cybernetics*, *46*, 474–486.
Xiong, C., Huang, J., & Lu, X. (2020). Framework for city-scale building seismic resilience simulation and repair scheduling with labor constraints driven by time–history analysis. *Computer-Aided Civil and Infrastructure Engineering*, 35, 322–341.
Xu, M., Ouyang, M., Mao, Z., & Xu, X. (2019). Improving repair sequence scheduling methods for postdisaster critical infrastructure systems. *Computer-Aided Civil and Infrastructure Engineering*, *34*, 506–522.
Yazdani, M., Aleti, A., Khalili, S. M., & Jolai, F. (2017). Optimizing the sum of maximum earliness and tardiness of the job shop scheduling problem. *Computers & Industrial Engineering*, *107*, 12–24.
Yazdani, M., Kabirifar, K., Fathollahi-Fard, A. M., & Mojtahedi, M. (2021). Production scheduling of off-site prefabricated construction components considering sequence dependent due dates. *Environmental Science and Pollution Research*, 1–17.
Yazdani, M., Mojtahedi, M., Loosemore, M., & Sanderson, D. (2022). A modelling framework to design an evacuation support system for healthcare infrastructures in response to major flood events. *Progress in Disaster Science*, *13*, 100218.
Yuan, G., Yang, Y., Tian, G., & Fathollahi-Fard, A. M. (2022). Capacitated multi-objective disassembly scheduling with fuzzy processing time via a fruit fly optimization algorithm. *Environmental Science and Pollution Research*. https://doi.org/10.1007/s11356-022-18883-y.
Zhang, Q., & Li, H. (2007). MOEA/D: A multiobjective evolutionary algorithm based on decomposition. *IEEE Transactions on Evolutionary Computation*, *11*, 712–731.
Zitzler, E., & Thiele, L. (1999). Multiobjective evolutionary algorithms: A comparative case study and the strength Pareto approach. *IEEE Transactions on Evolutionary Computation*, *3*, 257–271. https://doi.org/10.1109/4235.797969.
Zokaee, M., Tavakkoli-Moghaddam, R., & Rahimi, Y. (2021). Post-disaster reconstruction supply chain: Empirical optimization study. *Automation in Construction*, *129*, 103811. https://doi.org/10.1016/j.autcon.2021.103811.